Chapter 9

Preservation and reusability

Today's particle physics experiments are designed to collect physics data over a span of several decades. They operate at scales and complexities that make it impossible for the experiments to be repeated in the foreseeable future. The data taken at these experiments and physics results derived are thus exceptionally valuable and major problems arise from a scientific reproducibility point of view. In the following, reusability problems directly related to an individual analysis are discussed, and approaches taken in view of analysis preservation and reinterpretation are presented. This chapter starts with a brief motivation for reinterpretations, followed by a description of the main ingredients necessary. The remaining sections discuss three separate efforts aiming to improve the reinterpretability of the 1ℓ search in light of new signal models.

9.1 The case for reinterpretations

9.1.1 Motivation

Designing and executing searches for BSM physics requires a substantial amount of person-power and computing resources. As laid out in detail in part II of this thesis, an analysis generally aims to design signal regions in which a given BSM signal can be efficiently discriminated against SM background. Although the careful design of such regions already requires a significant amount of resources, it constitutes only a fraction of the work necessary for concluding the search. Contributions in the signal regions from SM processes need to be estimated, usually requiring expensive MC simulation and the development of background estimation strategies. Systematic uncertainties arising from numerous sources need to be considered and their impact estimated. For the BSM signal, a similar processing pipeline involving MC simulation, event reconstruction and event selection including uncertainties needs to be executed. Furthermore, recorded data also needs to be reconstructed and processed through the analysis-specific event selection. Only after the expected and observed event rates in all regions are known, can the statistical evaluation be performed.

As shown in fig. 9.1, an analysis can thus be divided into three main processing pipelines; a *background pipeline*, a *signal pipeline* and a *data pipeline*. After all three processing pipelines are concluded, the next analysis step can be performed—the *statistical inference*, producing the final analysis results, like quantifying excesses in data or setting limits on model parameters.

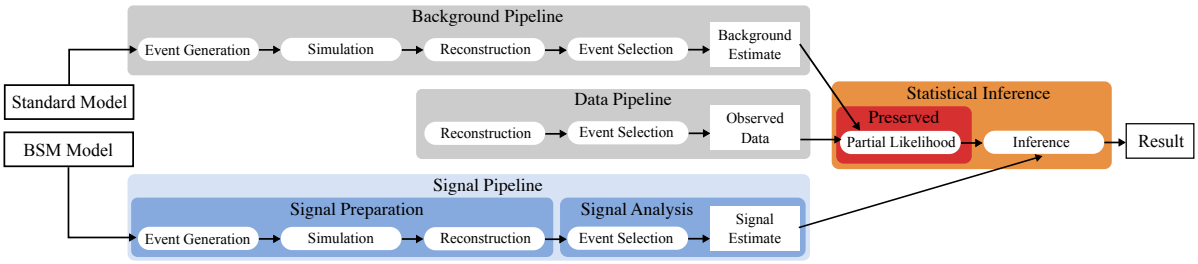

Figure 9.1: Full analysis workflow including the three main processing pipelines for deriving background and signal estimates as well as observed data rates. The outputs of the three processing pipelines are combined into a likelihood forming the basis for the statistical inference. In a RECAST setup (details in text), the estimated background rates and observed data are archived, and the signal pipeline is fully preserved, such that it can be re-executed with different inputs at any time. Figure recreated from Ref. [251].

Due to the substantial amount of resources necessary for developing and performing an analysis, it is not feasible to develop dedicated searches for every possible BSM scenario. Instead, analyses are typically only interpreted in a finite set of models with a small number of free parameters that need to be varied. Still, it is likely that a given analysis is sensitive to a variety of different BSM scenarios not considered in the original publication.

Consequently, it is not surprising that there is significant interest in the HEP community to reinterpret BSM searches in different signal models. Reinterpretations of ATLAS searches for SUSY are routinely performed by various reinterpretation efforts. In the context of direct constraints on BSM physics, the search results published by the experimental collaborations represent the only windows into the LHC data that are available to the wider HEP community. Reinterpretations of BSM searches are thus the only possibility to determine the implications of LHC data for a broad range of models [250].

As will be discussed in chapter 11, reinterpretations are not only of interest for the wider HEP community, but also for the experimental collaborations themselves. Within ATLAS, reinterpretations of SUSY searches can, for example, serve as powerful tools to state a comprehensive summary of ATLAS's sensitivity to SUSY models.

9.1.2 Approaches for reinterpretations

As the event selection of an analysis is fixed, the pre-fit background estimates and observed data in the regions of interest of the analysis do not change. Hence, the data and background pipelines shown in fig. 9.1, entering the statistical inference of the analysis by means of event rates, can be archived in a format significantly smaller than the original input data. In consequence, reinterpreting a search in the light of a new signal model requires the re-execution of two main analysis ingredients with (partially) new inputs; the signal pipeline and the statistical inference.

Recently, it has become possible to preserve the partial analysis likelihood[†] built from the background estimates and observed data, including all auxiliary data and details of the statistical model used for inference in a pure-text format [149]. In fig. 9.1, this is indicated through a red rectangle. Once the signal estimates are known, a new full analysis likelihood can be built, and

[†] As before, this only refers to likelihoods built using the HISTFACTORY template.

the viability of the new signal model can be tested with respect to the analysis in question. The publication of the likelihood of the 1ℓ search will be discussed further in section 9.2.

Different approaches can be taken for rendering the signal pipeline reusable to the extent that signal estimates for a new BSM scenarios of interest can be derived. Manifestly the most precise approach involves executing the original analysis software, but using a different BSM model as input. As this requires the preservation of the entirety of the original software environment, including the workflows used in the analysis, this is arguably the most involved approach, especially since it involves executing the computationally expensive detector simulation. A framework designed to facilitate such an effort, called RECAST and originally proposed in Ref. [252], is under development and aims to provide the cyber-infrastructure needed for offering *reinterpretations as a service*. Through a web interface, physicists wishing to reinterpret a search with RECAST, would provide an alternative BSM model and trigger a computational workflow that would re-execute the original analysis using the new signal inputs and ultimately deliver the *recasted* results. An attempt to fully preserve the 1ℓ search using the RECAST paradigm is discussed in section 9.3.

As the details of the existing RECAST implementations of ATLAS searches for SUSY are not publicly available, but only meant to be interacted with through a RECAST request, the exact implementation of the analysis selection is in general not available outside the ATLAS collaboration. For this reason, a number of public tools aiming to reimplement an approximated version of the event selections of a number of BSM searches at the LHC are available. Prominent examples include CHECKMATE [253, 254] and MADANALYSIS5 [255]. ATLAS has internally maintained a similar catalogue of its SUSY analyses and is publishing event selection snippets in C++ for many SUSY searches on HEPDATA [256], a repository for high energy physics data. Recently, this package maintained by ATLAS, called SIMPLEANALYSIS [257], has been made publicly available, allowing the C++ snippets published to be executed outside the collaboration.

A crucial step, necessary for achieving a reliable reimplementation of the signal pipeline, is the detector simulation. Executing the full detector simulation requires access to the collaborations's detector descriptio and is computationally expensive, disfavouring[†] its usage in the context of large-scale reinterpretations over a large set of models. For this reason, it is often approximated using simplified detector geometries and granularities. The most commonly used package for a fast detector simulation outside of the ATLAS collaboration is DELPHES [258], which is used in, e.g., CHECKMATE and MADANALYSIS5. Other packages like, e.g., RIVET [259, 260] approximate the detector response using dedicated four-vector smearing techniques, assuming that the detector response roughly factorises into the responses of single particles. Internally, ATLAS also maintains a dedicated framework for four-vector smearing, used in scenarios where other fast simulation techniques are still too expensive. Section 9.4.2 discusses these dedicated smearing functions further.

Finally, instead of trying to estimate the signal rates of a new model using MC simulation and (reimplemented) analysis event selections, some reinterpretation efforts like, e.g., SMODELS [261, 262], use *efficiency maps* encoding the selection and acceptance efficiencies of the analysis as a function of the model parameters (typically the sparticle masses in the case of SUSY searches) and analysis selections. Such efficiency maps are routinely published on HEPDATA by ATLAS

[†] This is especially true for reinterpretation efforts outside the ATLAS collaboration, which cannot make use of the collaboration's detector description.

SUSY searches, and allow for efficient reinterpretations, as long as the signal efficiencies mostly depend on the signal kinematics and are largely independent from the specific details of the signal model [261]. For the 1ℓ search presented herein, the efficiency maps, including additional analysis data products, are available at Ref. [263].

9.2 Public full likelihood

The likelihood is arguably one of the most information-dense and important data products of an analysis. If the exact likelihood function of the original analysis is not known in reinterpretation efforts[†], approximations need to be made for the statistical inference, e.g. in terms of the correlations between event rate estimates as well as the treatment of uncertainties. Recently, ATLAS has started to publish full analysis likelihoods built using the HistFactory pdf template [149]. This effort has been facilitated by the development of `pyhf` (cf. section 3.1), in conjunction with the introduction of a `JSON` specification fully describing the HistFactory template. As a pure-text format, the `JSON` likelihoods are human- and machine-readable, highly compressible and can easily be put under version control, all of which are properties that make them suitable for long-term preservation, which is a crucial condition for reinterpretations.

The full likelihood of the 1ℓ search is publicly available at Ref. [264] and is not only heavily used in the following chapters, but also in various analysis reinterpretation and combination efforts currently ongoing in ATLAS. Several efforts outside of the ATLAS collaboration have already included the analysis likelihood into their reinterpretations, and the SModelS [265] and MadAnalysis5 [266, 267] collaborations have both reported significant precision improvements through its use. Furthermore, the full likelihood of the search presented herein has recently been used to demonstrate the concept of scalable distributed statistical inference on high-performance computers (HPCs) [268]. Through the `funcX` package [269], `pyhf` is used as a highly scalable *function as a service* to fit the entire 1ℓ signal grid of 125 signal points with a wall time of 156 s using 85 available worker nodes[§].

9.3 Full analysis preservation using containerised workflows

For an analysis to be fully reusable under the Recast paradigm, the signal pipeline of the original analysis (cf. fig. 9.1) needs to be preserved such that it can be re-executed on new inputs. As typically only the processing steps after the event reconstruction are analysis-specific, it is sufficient to preserve this part of the signal pipeline. Processing steps including and preceding the event reconstruction only involve the central ATLAS production system, introduced in section 2.2.8, and result in an ATLAS-internal data format serving as input for physics analyses. These processing steps are preserved using centrally provided ATLAS infrastructure and thus do not need to be within the scope of the preservation discussed in the following.

[†] Up until recently, the exact likelihood function was not part of the data products published by ATLAS searches for SUSY, hence approximations of the statistical models were a crucial part of most reinterpreation efforts.

[§] Theses benchmarks use `pyhf`'s NumPy backend and SciPy optimiser, a combination that has a slower log-likelihood minimisation time than e.g. PyTorch coupled with SciPy, as will be shown in section 10.3.

In the following, the term *signal analysis* (cf. fig. 9.1) will refer to the analysis-specific processing steps that are not handled by the central ATLAS production system, typically starting with the selection of events that have passed the reconstruction step in fig. 9.1, provided in the aforementioned internal data format. Preserving the signal analysis not only needs preservation of the full software environment required for the different processing steps, but also knowledge of the correct usage of the software through parameterised job templates together with a workflow graph connecting the different processing steps. A graph representation of the entire analysis, implemented in RECAST is shown in fig. 9.2.

9.3.1 Software preservation

As much of the software is only tested, validated and deployed on a narrow set of architectures and platforms, the full software environment defining an analysis pipeline not only includes the original analysis-specific code used for object definitions, calibrations, event selection and statistical inference, but also the operating system used, and a number of low-level system libraries that the applications depend upon. Preserving the full software environment can be achieved through the use of *Docker containers* [270, 271], a technology that—except for the operating system kernel—packages the full software environment in a portable data format, including a layered file system, the operating system as well as the actual application and all of its dependencies. As opposed to full virtualisation, Docker containers do not rely on actual hardware virtualisation but share the operating system kernel with the host. As such, they only interact with the host through system calls to the Linux kernel [271], offering a highly stable interface. This makes Docker containers a well-suited solution for deploying isolated applications on a heterogeneous computing infrastructure.

Due to the specific software structure of the 1ℓ search, a containerisation requires a total of three container images. Two images contain the software necessary for performing the physics object calibrations and event selection, as well as the conversion of the information in a format that can be used by the downstream steps. The third image contains the software necessary for the statistical inference, relying on the `pyhf`-implementation of the HISTFACTORY models in order to benefit from the possibility of using a partial `JSON` likelihood to preserve background and data rates.

The Docker images are built from suitable base images containing the software environment used for deriving the published 1ℓ search results, expanded with the relevant analysis software. All docker images are subject to version control and continuous integration, such that changes to the underlying software environment can be tracked and tagged. This allows for a consistent preservation of multiple versions of the analysis pipeline.

9.3.2 Processing steps preservation

Preserving the software environment is not sufficient, as detailed instructions on how to use it have to be given. This is achieved through parameterised job templates that specify the precise commands and arguments required to re-execute the analysis code for specific processing steps. As re-executing the analysis pipeline using different signal models involves varying input parameters, all job template parameters are exposed to the user. In fig. 9.2, the parameterised

job templates including their output are shown as blue rectangles, connected together through a workflow specification represented via black arrows.

User-specifiable arguments and inputs to the event selection and physics object calibration step include the actual reconstructed MC events in the aforementioned ATLAS-internal format, obtained through the central ATLAS production system, as well as corresponding files necessary for the pile-up correction in MC. In addition, the signal process cross section as well as MC generator-level efficiencies need to be given for the correct normalisation of the estimated signal rates to the integrated luminosity of the full Run 2 dataset. For each new signal model to be tested, three MC samples need to be provided, generated with specific pile-up profiles close to the pile-up profile in data during the 2015–2016, 2017 and 2018 data-taking periods, respectively[†]. In all three jobs, the events processed are weighted according to the integrated luminosity of the data-taking period they represent within the full Run 2 dataset. A subsequent *merging* step uses the same docker image as the previous processing step, and serves to merge the three produced outputs into a single ROOT file that can be read by the subsequent step.

In addition, a `JSON` file containing theory uncertainties on the expected signal rates can be provided. These are optional and do not have to be specified if deemed to be negligible for the signal model under consideration.

The statistical inference step requires, as external input, the archived partial likelihood containing observed data as well as expected background rates including systematic variations thereof. This step generates a new full analysis likelihood and performs the necessary hypothesis tests.

9.3.3 Workflow preservation

Finally, the preserved processing steps need to be linked together, creating a parameterised workflow completely defining the analysis pipeline, starting from centrally produced MC datasets up to the statistical inference results. Within Recast, this is achieved using the workflow description language `yadage` [272], capturing the full workflow in `YAML` format. The workflow uses the job templates and defines their processing order and dependencies.

The Recast implementation of the analysis presented in this work has been validated against original analysis inputs. The expected and observed CL_s values derived in the original analysis were successfully re-derived using the containerised workflow implementation. On a non-isolated CPU, the full preserved analysis pipeline for a single signal model can be executed with a wall time of about 50 min. Due to the highly portable nature of the containerised workflow, the pipeline can easily be run in a distributed setup, allowing scalable reinterpretations at full analysis precision.

[†] This allows to have pile-up weights relatively close to unity, avoiding unnecessary statistical dilution.

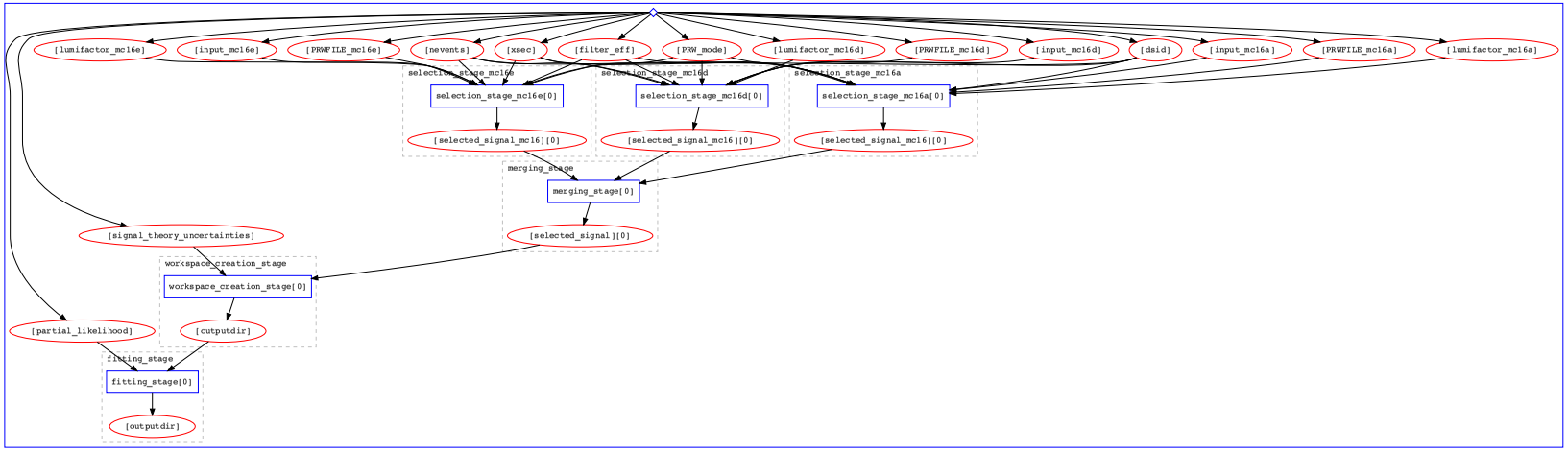

Figure 9.2: Graph of the workflow as specified for the analysis pipeline. The containerised processing steps are represented as blue rectangular nodes, while input parameters, input files and outputs are shown as red oval nodes. The workflow is comprised of four processing steps: `selection_stage_mc16(a,d,e)`, `merging_stage`, `workspace_creation_stage` and `fitting_stage`. The first two steps perform the object calibration, event selection and merging of the three MC datasets representing the three data-taking periods 2015–2016, 2017 and 2018. The latter two steps implement the generation of the signal `JSON` patch as well as the final statistical inference. Compared to fig. 9.1 the first two steps implement the *signal analysis* part, while the latter two steps implement the *statistical inference* deriving the final results.

9.4 Truth-level analysis

A full preservation of the entire analysis pipeline, as presented in the previous section, is highly desirable as it allows for a maximum precision reinterpretation of the original analysis using a new BSM model. As the full detector simulation needs a significant amount of computing resources in addition to the non-negligible wall time of the actual preserved analysis pipeline, this approach can only be used on a limited set of models. In large-scale reinterpretations over high-dimensional parameter spaces, the amount of models that need to be sampled and investigated using the analysis is too high to employ the fully preserved analysis pipeline in every case. In order to significantly reduce the number of models that need to be passed through the full analysis pipeline, a pre-sorting of the models needs to be performed, filtering models for which (non-)exclusion based on a simplified analysis implementation is uncertain.

In the following, two major, complementary approaches to analysis simplifications are discussed, targeting both the *signal pipeline* as well as the *statistical inference* blocks in fig. 9.1. This section discusses the SimpleAnalysis implementation of the analysis, an approach implementing the signal pipeline at *truth-level*, i.e. using the generator-level objects without running a dedicated detector simulation. An approximation of the detector response using four-vector smearing techniques is discussed.

The second simplification is discussed in chapter 10, introducing a procedure for building simplified likelihoods from the full likelihoods of ATLAS SUSY searches in order to significantly lower the wall time needed for the statistical inference. In chapter 11, both approximations are combined and applied on a set of SUSY models sampled from the pMSSM.

9.4.1 Truth-level selection

All signal and control regions considered in the original 1ℓ search are implemented at truth-level using the publicly available framework SimpleAnalysis. The exact implementation has been published, together with the previously discussed efficiency maps and analysis likelihod, as part of the auxiliary analysis data at Ref. [263]. In fact the SimpleAnalysis implementation of the search was already used in chapter 7 for the derivation of some of the theory uncertainties.

The truth-level implementation explicitly specifies all object definitions introduced in section 4.4, even though some of them, like the lepton isolation, are technically not well-defined at truth-level. The four-vector smearing subsequently described is, however, in many cases implemented as a function of said object definitions and hence still allows to consider them to some extent. Additionally, as discussed in section 9.1, the full specification of the original analysis event selection including all object definitions allows for more straightforward reinterpretations by efforts outside of the ATLAS collaboration that generally do not have access to the original analysis software.

Following the object definitions, an overlap removal procedure following the same prescription as described in section 4.5 for the reconstruction-level analysis is performed, i.e. especially also using the same shrinking cone definitions. Since tracking information is not available at truth-level, the overlap removal step removing electrons sharing a track with a muon is approximated by using a distance parameter of $\Delta R = 0.01$ between the objects. Although often

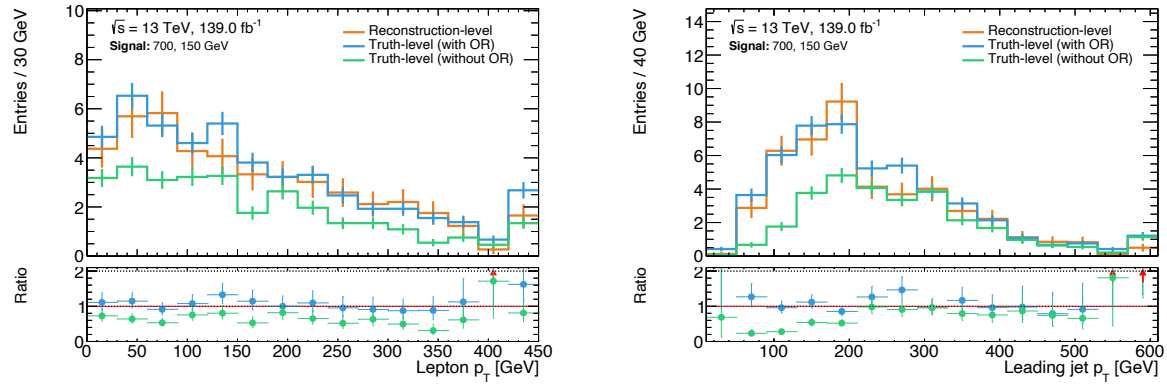

Figure 9.3: Impact of the overlap removal (OR) procedure at truth-level illustrated in the lepton and leading jet transverse momenta distributions. The truth-distributions with (blue) and without (green) overlap removal (green) are compared with a reconstruction-level (orange) distribution. The exemplary benchmark signal point with $m(\tilde{\chi}_1^{\pm}/\tilde{\chi}_2^0), m(\tilde{\chi}_1^0) = 700, 150\,\text{GeV}$ is shown in both plots. Both truth-level distributions are shown after smearing. All distributions are shown in a loose preselection requiring exactly one lepton, $E_{\text{T}}^{\text{miss}} > 50\,\text{GeV}$, $m_{\text{T}} > 50\,\text{GeV}$, and 2–3 jets, two of which need to be b-tagged.

neglected[†] in reinterpretation efforts outside of the collaboration, the correct implementation of the overlap removal procedure employed in the original analysis is crucial to reproduce the signal estimates of the original analysis. Figure 9.3 illustrates this by showing exemplary kinematic distributions of an exemplary signal point in configurations with and without overlap removal at truth-level, and comparing it with the distributions obtained at reconstruction-level[§]. Not implementing the overlap removal procedure of the original 1ℓ search, results in many truth-level events not passing the analysis selections because of additional objects in the final state that would otherwise have been removed through the overlap removal.

Finally, the exact implementation of all analysis observables is explicitly given, followed by the definition of all control and signal regions.

9.4.2 Truth smearing

The general assumption of the truth smearing applied in the following is that the detector response roughly factorises into the responses of single particles. This allows to use the ATLAS detector performance results in order to construct detector response maps parameterised in different observables for each physics object. Detector response maps include object reconstruction and identification efficiencies as well as scale factors to correct for differences between MC and observed data. Likewise, effects from the finite resolution of energy measurements in the detector are modelled through energy resolution maps. In the following, the four-vector components of electrons, muons, jets and $E_{\text{T}}^{\text{miss}}$ are smeared.

[†] The overlap removal procedures in ATLAS SUSY searches tend to be quite intricate, making them non-trivial to re-implement without ATLAS and analysis-specific knowledge.

[§] The term *reconstruction-level* here refers to distributions obtained with MC simulated datasets for which the full detector simulation and reconstruction has been run.

In the case of truth electrons, the identification efficiencies considered are parameterised in η and p_{T} as well as the identification working point used [212]. In η, nine fixed-width bins are used. In p_{T}, six bins are implemented and a linear interpolation between two adjacent p_{T}-bins is used to get the efficiency for the given p_{T} of each truth electron. The probability of finding a fake electron in a truth jet is estimated through a similar two-dimensional map depending on the truth jet η and p_{T}, again using fixed-width bins in η and a linear interpolation in p_{T}. The range of the p_{T} interpolation for identification efficiencies and fake rates extends from 7 GeV to 120 GeV, covering the majority of all electrons in the analysis. If the truth p_{T} of the electron is outside of that range, the identification efficiency and fake rate from the respective bound of the corresponding η-bin are used. The probability for misidentifying an electron as a photon is estimated using different fixed values for the barrel and end-cap regions [211]. Finally, the transverse energy of the electron is smeared using a random number drawn from a Gaussian distribution with standard deviation corresponding to the η- and p_{T}-dependent energy resolution, measured in $Z \to ee$ and $J/\Psi \to ee$ events [273].

For truth muons, the identification efficiencies are also parameterised in η and p_{T} as well as the identification working point used [214]. Similar to truth electrons, the p_{T} of the muon is smeared using a Gaussian distribution with standard deviation corresponding to the momentum resolution. The momentum resolution of combined truth muons, σ_{CB}, is computed from the resolutions in the ID, σ_{ID}, and MS, σ_{MS}, as

$$\sigma_{\mathrm{CB}} = \frac{\sigma_{\mathrm{ID}}\sigma_{\mathrm{MS}}}{\sqrt{\sigma_{\mathrm{ID}}^2 + \sigma_{\mathrm{MS}}^2}}, \tag{9.1}$$

where σ_{ID} and σ_{MS} are parameterised in η and p_{T} and measured in $Z \to \mu\mu$ and $J/\Psi \to \mu\mu$ events [213].

The transverse momentum of truth jets is smeared using a Gaussian with standard deviation equal to the JER, provided in a map parameterised in five bins in $|\eta|$, ranging from $|\eta| = 0$ to $|\eta| = 4.5$. The jet energy resolutions are measured in dijet events [218] and provided as parameterisations of a noise N, stochastic S and constant C term for each of the seven bins in $|\eta|$, such that the resolution can be computed as

$$\frac{\sigma(p_{\mathrm{T}})}{p_{\mathrm{T}}} = \frac{N}{p_{\mathrm{T}}} \oplus \frac{S}{\sqrt{p_{\mathrm{T}}}} \oplus C. \tag{9.2}$$

Only truth jets with $10\,\mathrm{GeV} < p_{\mathrm{T}} < 1.5\,\mathrm{TeV}$ are smeared. For truth jets with $p_{\mathrm{T}} > 20\,\mathrm{GeV}$, the flavour tagging efficiency is considered using efficiencies parameterised in η, p_{T} and the MV2c10 efficiency working point (introduced in section 4.4) used, measured in fully reconstructed simulated $t\bar{t}$ events [224].

Finally, the smeared missing transverse energy is computed using the transverse momenta of all smeared truth objects in the event, including an approximation for the track soft term. The latter is approximated using resolution measurements from $Z \to \ell\ell$ events [227], allowing to infer a distribution of the mean soft term projected in the direction longitudinal to the total transverse momentum of all hard objects in an event, $\boldsymbol{p}_{\mathrm{T}}^{\mathrm{hard}}$. The measured resolution parallel and perpendicular to $\boldsymbol{p}_{\mathrm{T}}^{\mathrm{hard}}$ is then used to smear the nominal soft track value.

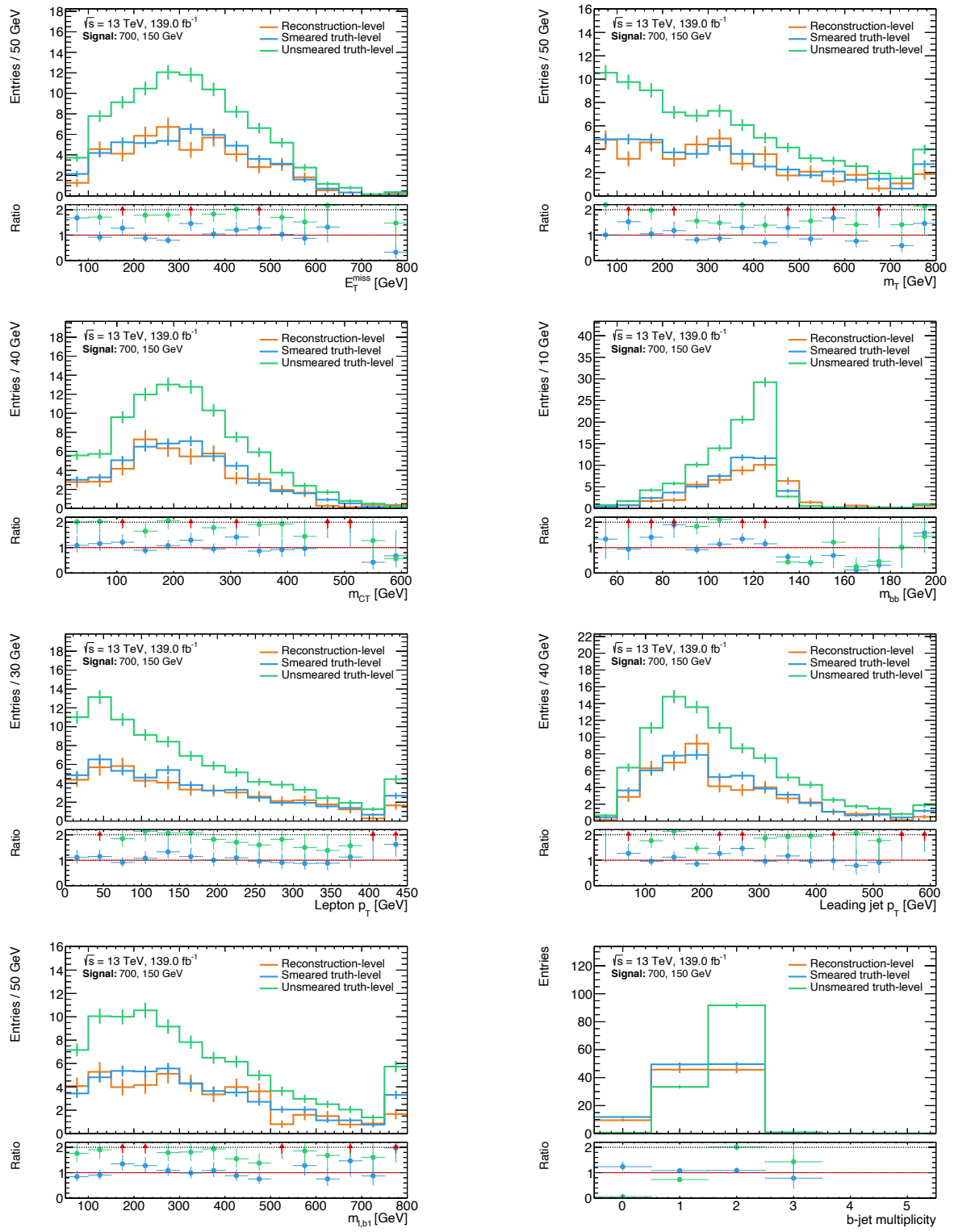

Figure 9.4: Comparisons of the kinematic distributions of key observables at (smeared) truth- and reconstruction-level. The exemplary benchmark signal point with mass parameters $m(\tilde{\chi}_1^{\pm}/\tilde{\chi}_2^0), m(\tilde{\chi}_1^0) = 700, 150\,\text{GeV}$ is shown. The ratio pad shows the ratio of smeared and unsmeared truth-level distributions (blue and green) to reconstruction-level distributions (orange). Only MC statistical uncertainty is included in the error bars. All distributions are shown in a loose preselection requiring exactly one lepton, $E_{\text{T}}^{\text{miss}} > 50\,\text{GeV}$, $m_{\text{T}} > 50\,\text{GeV}$, and 2–3 jets, two of which need to be b-tagged. The latter requirement is dropped for the b-jet multiplicity distribution.

9.5 Validation of the truth-level analysis

9.5.1 Validation in loose preselection

The performance of the truth smearing is illustrated in fig. 9.4 in a loose preselection for an exemplary benchmark signal point. The loose preselection applied requires a final state with exactly one lepton, $E_{\mathrm{T}}^{\mathrm{miss}} > 50\,\mathrm{GeV}$, $m_{\mathrm{T}} > 50\,\mathrm{GeV}$, and 2–3 jets, two of which need to be b-tagged. The reconstruction-level distributions are compared with the truth-level distributions before and after truth smearing. It can be observed that the truth smearing noticeably improves the agreement between the truth- and reconstruction-level distributions. While the lepton and jet reconstruction and identification efficiencies are—due to their dependence on η, p_{T} and individual working points—crucial for the overall agreement in shape, especially at low p_{T}, the inclusion of flavour-tagging efficiencies significantly improves the overall agreement in normalisation.

Although some minor differences remain, a good agreement is observed overall across the relevant kinematic distributions at loose preselection level. Most of the differences remaining between smeared truth-level and reconstruction-level distributions in individual bins are well within the MC statistical uncertainties arising from the relatively limited MC statistics available.

9.5.2 Validation in signal regions

As the expected signal rates in the signal regions are ultimately what is entering the statistical inference, it is important that the good agreement observed at preselection is still present in the kinematically tighter selections of the signal regions. Additionally, it is worth investigating the agreement across all signal models considered in the original analysis, as opposed to only validating specific benchmark points. A comparison of the reconstruction-level and truth-level event rates before and after smearing in the signal regions SR-LM, SR-MM and SR-HM for all signal models considered in the 1ℓ search is shown in fig. 9.6. For the sake of conciseness, only the cumulative m_{CT} bins are shown in each signal region in fig. 9.6. The agreement in the individual m_{CT} bins in each SR-LM, SR-MM and SR-HM is provided in figs. B.1 to B.3.

The truth smearing drastically improves the agreement in event rate estimates at truth- and reconstruction-level across all SR bins. While, compared to reconstruction-level, the event rates are generally overestimated at truth-level before smearing, both tend to agree well within statistical uncertainties after smearing.

9.5.3 Validation using likelihood

Using the nominal expected event rates at (smeared) truth-level for every signal model in the original signal grid considered in the 1ℓ search, expected and observed CL_s values can be computed and exclusion contours can be derived. Figure 9.6 compares the expected and observed exclusion contours obtained using the full likelihood and reconstruction-level signal inputs with those obtained using the full likelihood and truth-level signal inputs before and after truth smearing. While all systematic uncertainties on the signal are included in the reconstruction-level contours, no signal uncertainties are considered when obtaining both the smeared and unsmeared truth-level contours. As expected from the previous validation steps

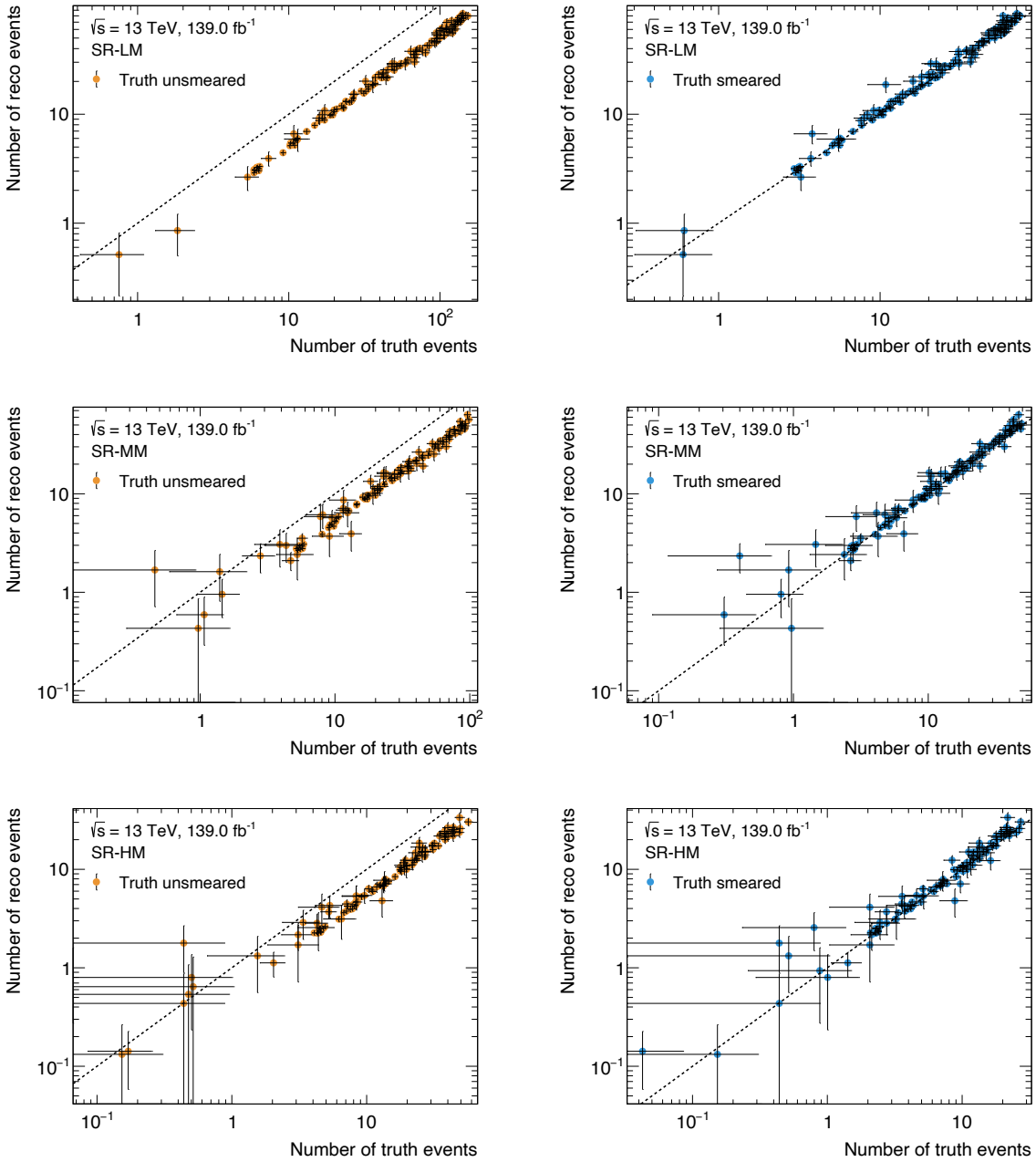

Figure 9.5: Comparison of the event rates at truth- and reconstruction-level before (left) and after (right) truth smearing. From top to bottom, the SR-LM, SR-MM and SR-HM signal regions are shown, with cumulative (integrated) m_{CT} bins. Every single point in the scatter plots represents a single signal model considered in the 1ℓ search. Uncertainty bars include MC statistical uncertainties.

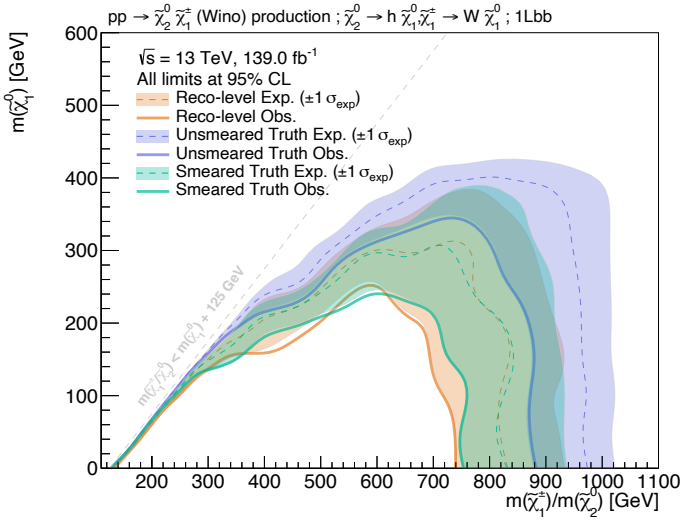

Figure 9.6: Expected and observed exclusion contours obtained with the full likelihood using reconstruction-level inputs (orange) as well as truth-level inputs before (purple) and after (green) smearing. Uncertainties include all statistical and systematic uncertainties on the background and signal for the reconstruction-level contours, but only statistical and systematic uncertainties on the background for truth-level signal inputs.

in the signal regions, the sensitivity using unsmeared truth-level signal inputs is significantly overestimated compared to the published analysis exclusion limit using reconstruction-level inputs. The smeared truth-level inputs, however, yield exclusion contours with an acceptable match compared to the reconstruction-level results.

In summary, the validation process performed at multiple selection levels of the analysis shows that the signal pipeline can be approximated reasonably well using a truth-level analysis and dedicated smearing functions. For signal models producing final states with kinematics close to those of the scenarios validated in the previous sections, this approach allows to determine the event rate estimates with high computational efficiency. In large-scale reinterpretations, the smeared truth-level analysis can be used as a basis for an efficient classification of models into two categories: models that are safely excluded or not excluded based on truth-level analysis only, and models where exclusion is in doubt and instead the precision of the full analysis pipeline using RECAST is required.

Appendix B

B.1 Truth smearing

The estimated event rates in the exclusion signal regions at truth-level before and after truth smearing are compared with the reconstruction-level event rates in figs. B.1 to B.3. Each one of the 125 signal models from the simplified model signal grid corresponds to one point in the scatter plots. The smearing significantly improves the agreement between truth- and reconstruction-level event rate estimates in all signal region bins.

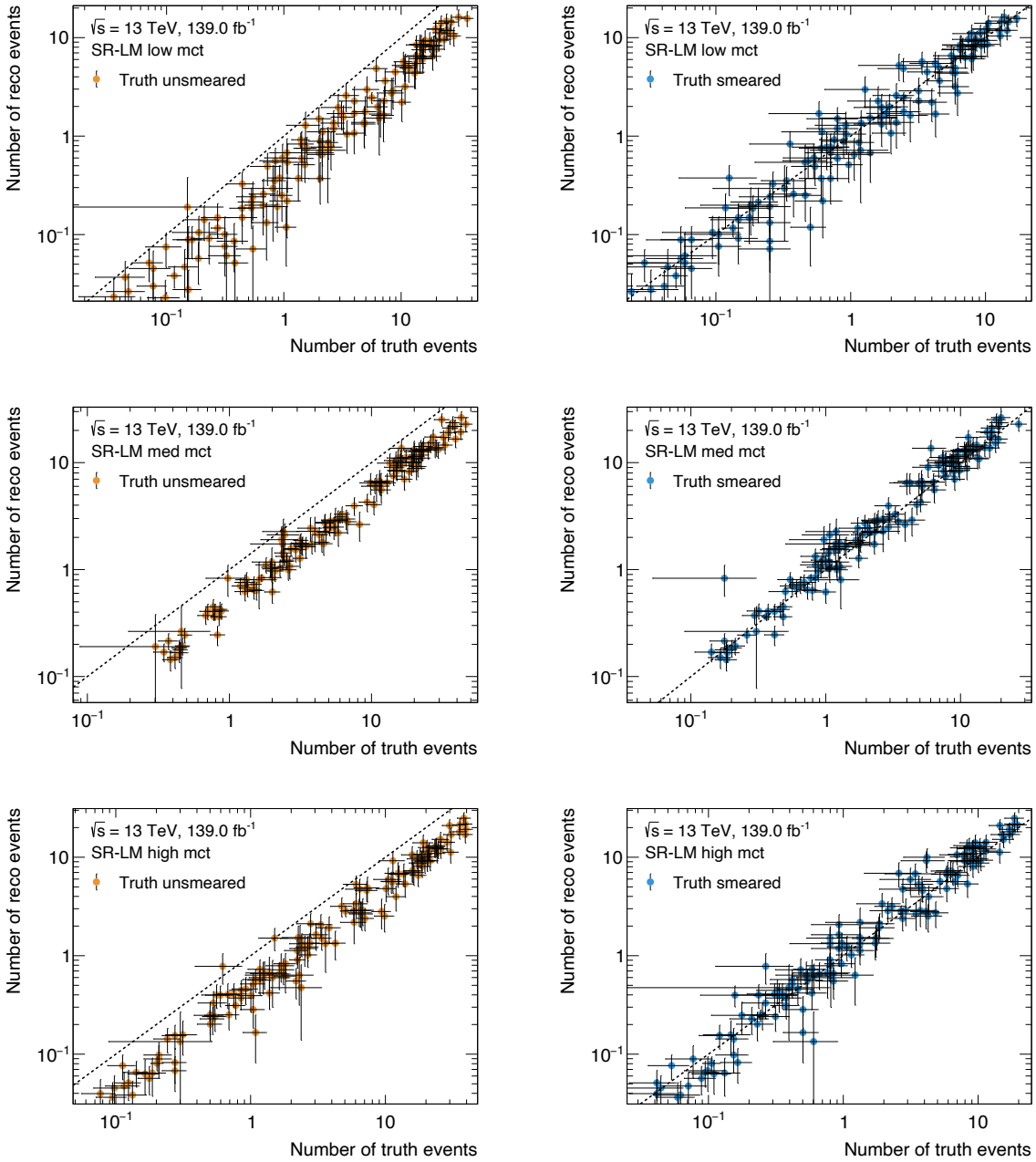

Figure B.1: Comparison of the event rates at truth- and reconstruction-level before (left) and after (right) truth smearing in SR-LM. From top to bottom, the low, medium and high m_{CT} bins are shown. Every single point in the scatter plots represents a single signal model considered in the original 1-lepton analysis. Uncertainties include only MC statistical uncertainties.

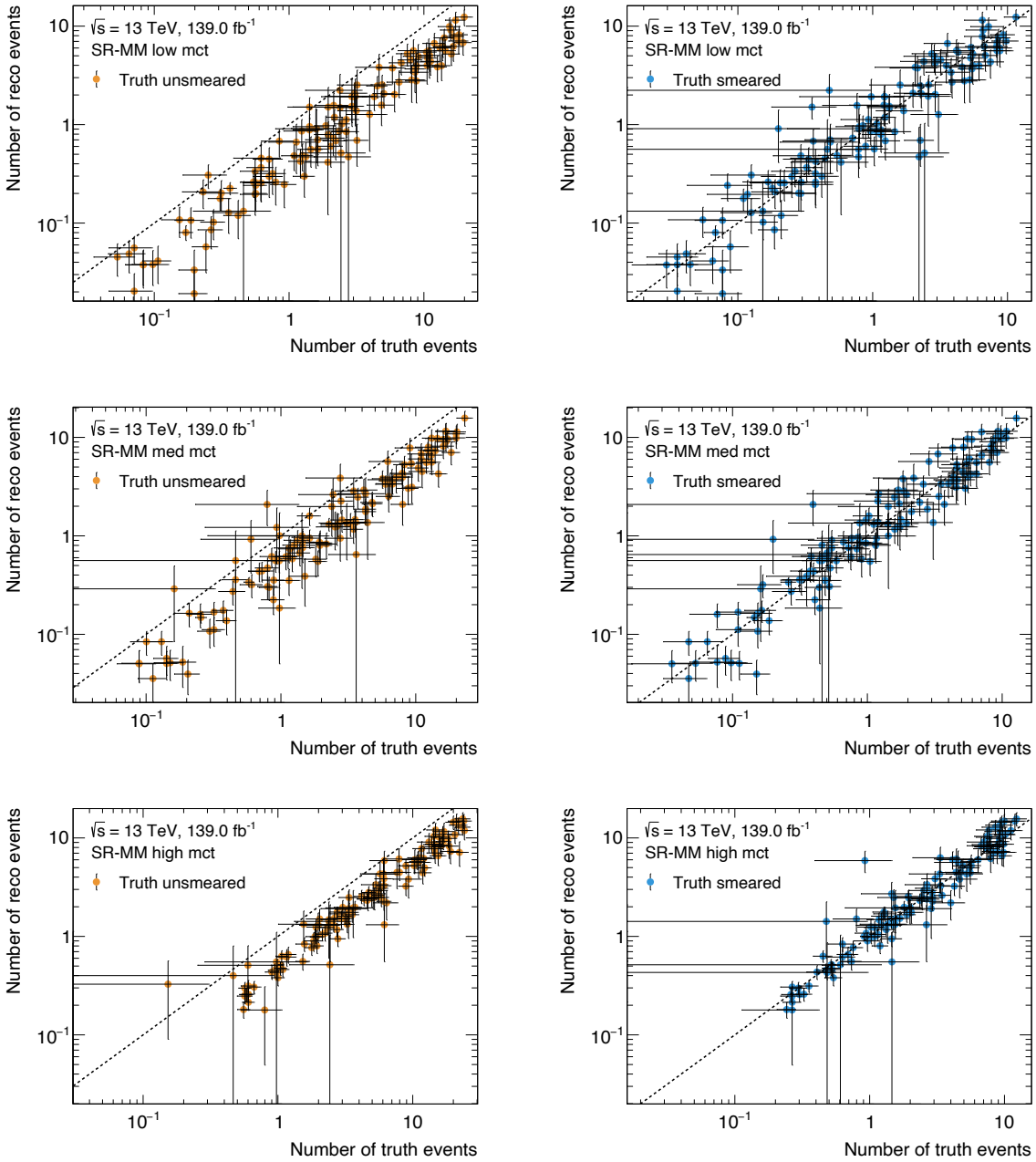

Figure B.2: Comparison of the event rates at truth- and reconstruction-level before (left) and after (right) truth smearing in SR-MM. From top to bottom, the low, medium and high m_{CT} bins are shown. Every single point in the scatter plots represents a single signal model considered in the original 1-lepton analysis. Uncertainties include only MC statistical uncertainties.

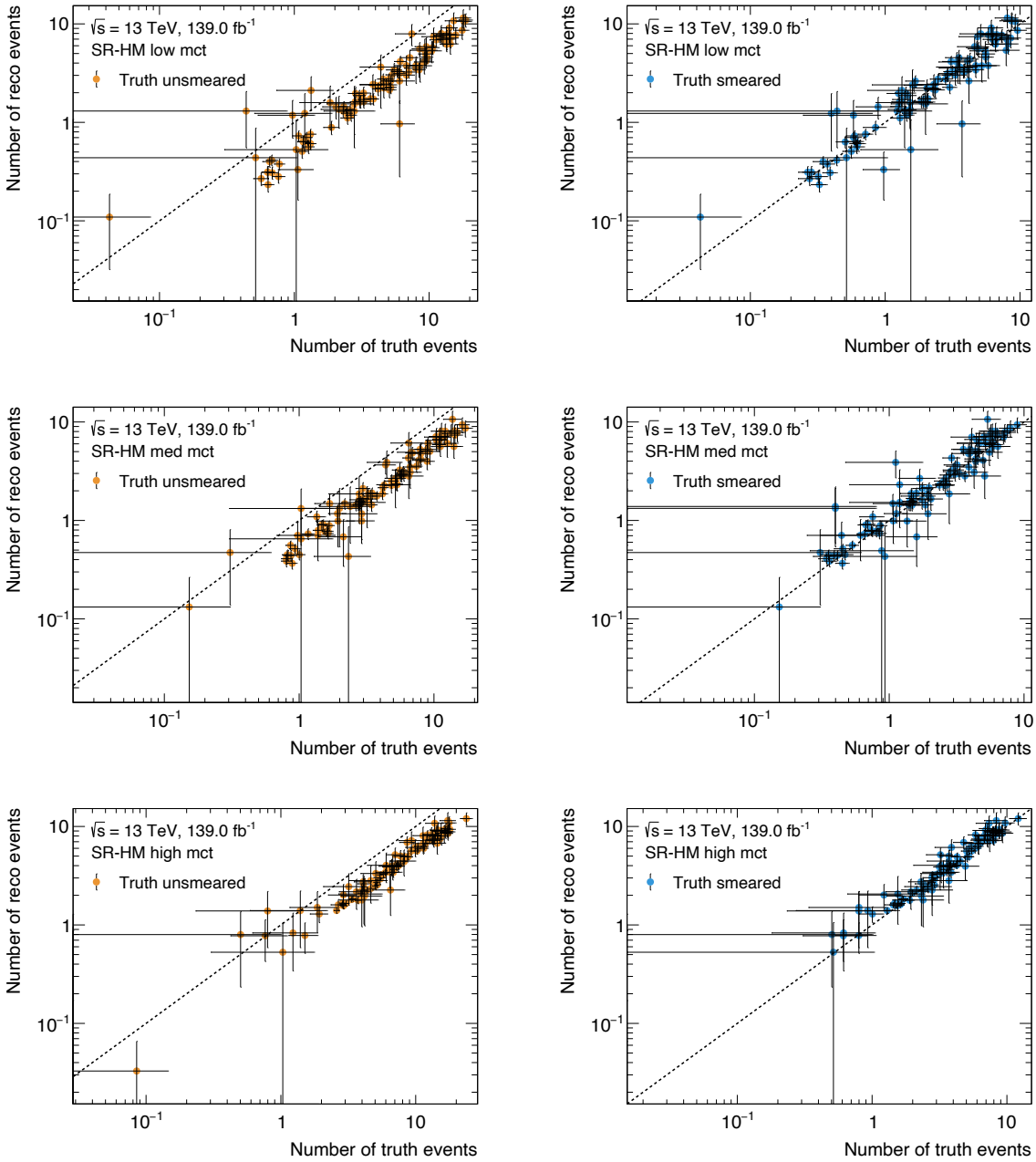

Figure B.3: Comparison of the event rates at truth- and reconstruction-level before (left) and after (right) truth smearing in SR-HM. From top to bottom, the low, medium and high m_{CT} bins are shown. Every single point in the scatter plots represents a single signal model considered in the original 1-lepton analysis. Uncertainties include only MC statistical uncertainties.

B.2 Simplified likelihood results

Figures B.4 and 10.5 show comparisons of the exclusion limits obtained using the full and simplified likelihoods for different ATLAS SUSY searches. In addition to the exclusion limits, the observed CL_s are given for every signal model tested. Although some likelihood simplifications needed special care (see section 10.5) and validation, a good agreement is observed throughout all analyses tested. Figures B.6 and B.7 directly compare the expected and observed CL_s values obtained using both likelihood configurations for each ATLAS SUSY search considered. Both linear- and log-scale representations are shown, revealing that the simplified likelihood tends to lead to good agreement in the CL_s values around 0.05, while slightly overestimating sensitivity in the region with $CL_s \ll 0.05$, where signal models are in any case being excluded (and thus to some extent it is not important how small the CL_s value actually is).

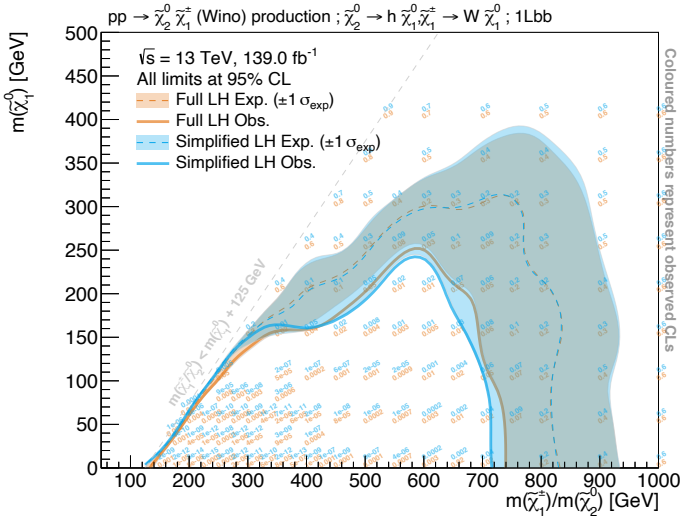

Figure B.4: Comparison of the simplified likelihood (blue contours) and full likelihood (orange contours) results for the search for electroweakinos presented previously. The observed contours are shown as solid lines, while the expected contours are shown as dashed lines. Observed CL_s values from both likelihoods are given. The uncertainty band includes all MC statistical and systematic uncertainties in the case of the full likelihood, and the simplified uncertainties in the case of the simplified likelihood.

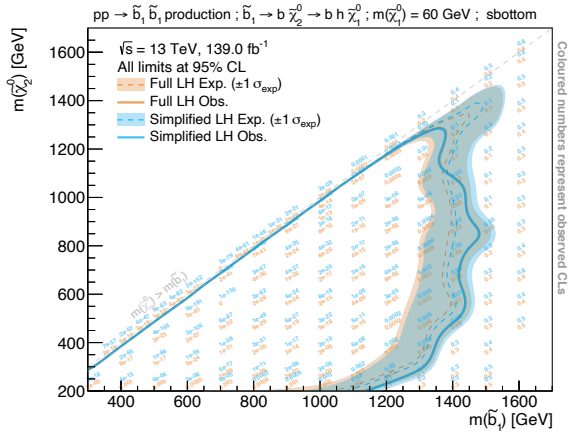

(a) ATLAS sbottom search [276]

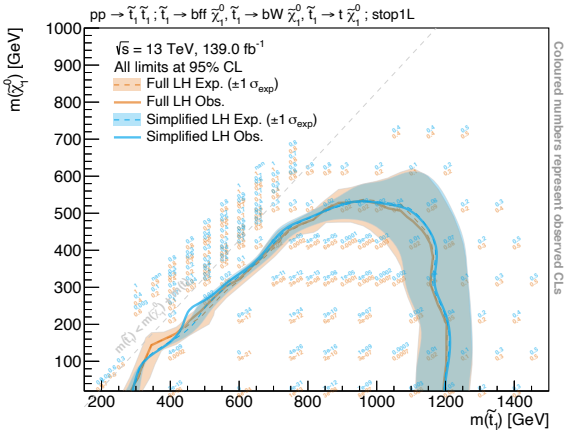

(b) ATLAS stop search

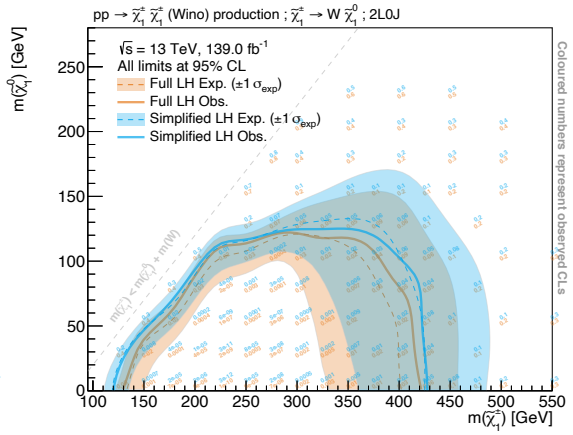

(c) ATLAS 2-lepton search [248]

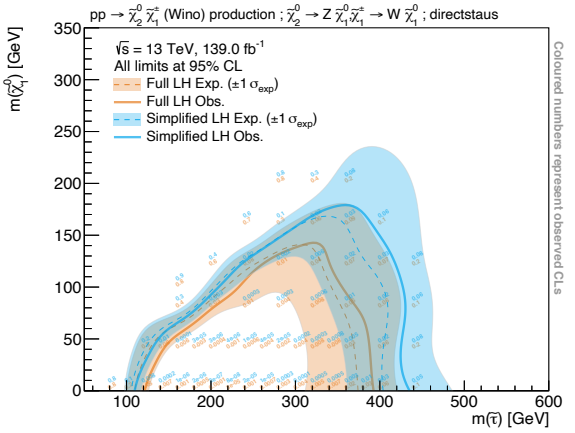

(d) ATLAS direct stau search [275]

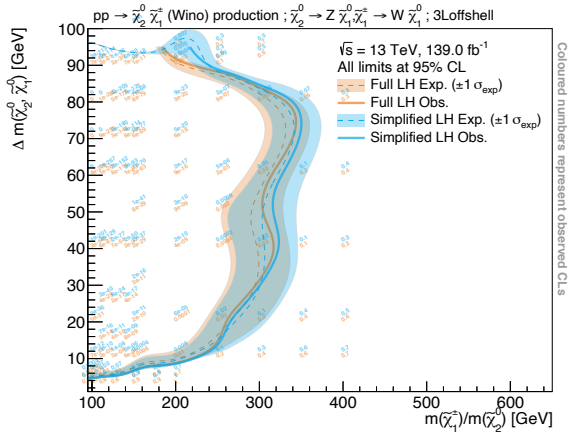

(e) ATLAS 3-lepton search

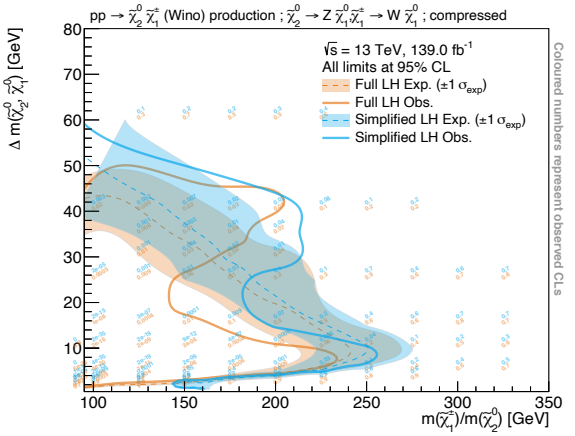

(f) ATLAS compressed search [274]

Figure B.5: Comparison of the simplified likelihood (blue contours) and full likelihood (orange contours) results for different ATLAS SUSY searches. The observed contours are shown as solid lines, while the expected contours are shown as dashed lines. Observed CL_s values from both likelihoods are given. The uncertainty band includes all MC statistical and systematic uncertainties in the case of the full likelihood, and the simplified uncertainties in the case of the simplified likelihood.

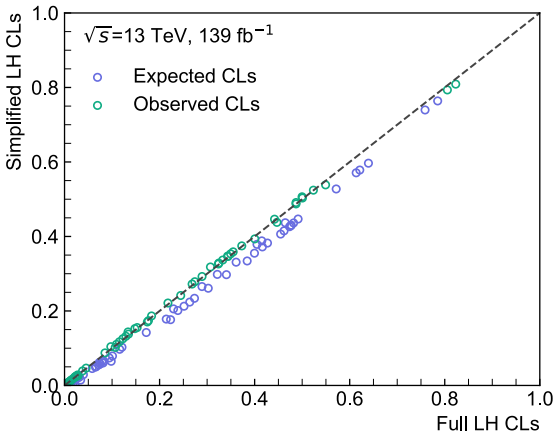

(a) ATLAS sbottom search [276]

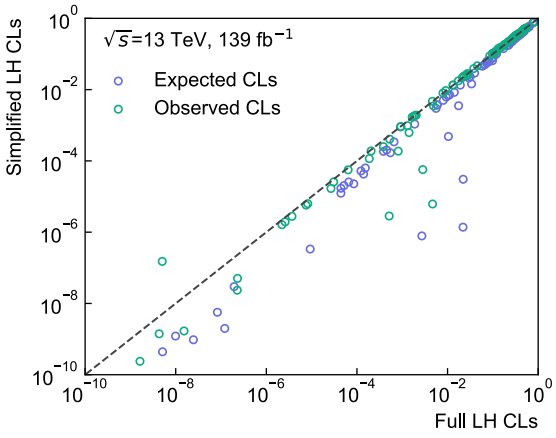

(b) ATLAS sbottom search [276]

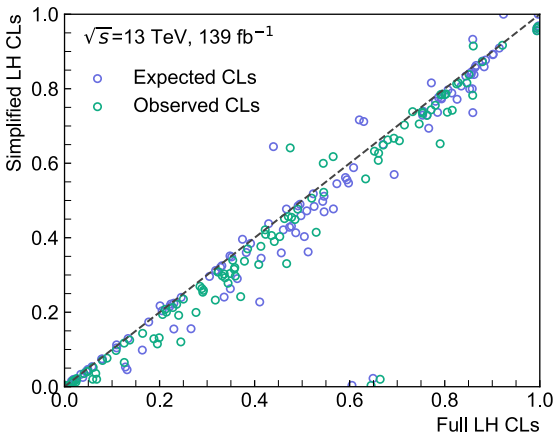

(c) ATLAS stop search

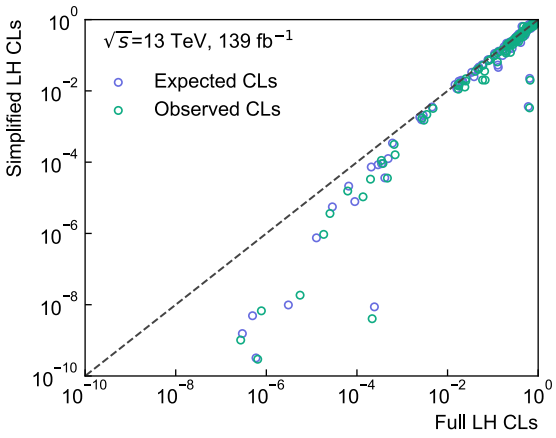

(d) ATLAS stop search

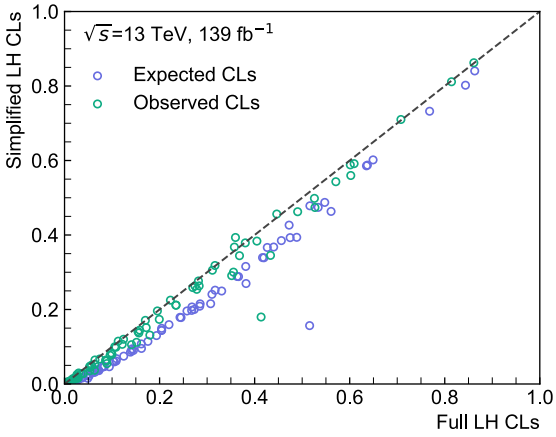

(e) ATLAS 2ℓ search [248]

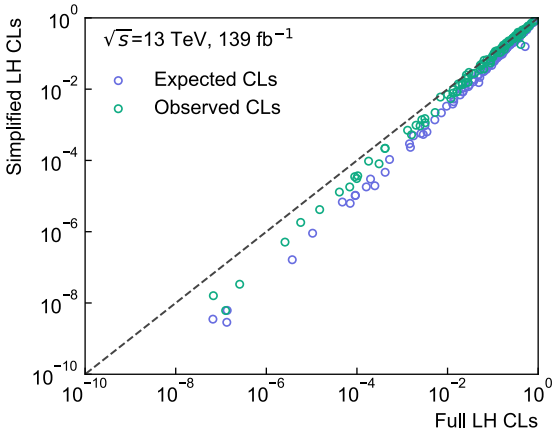

(f) ATLAS 2ℓ search [248]

Figure B.6: Scatter plots comparing the observed and expected CL_s values obtained using the simplified and the full likelihoods for the same set of signal models originally considered in the various ATLAS SUSY searches. Both linear and logarithmic scale representations are shown on the left- and right-hand side, respectively, illustrating the full range of CL_s values. Apart from the scales, both columns show exactly the same results for each row of plots.

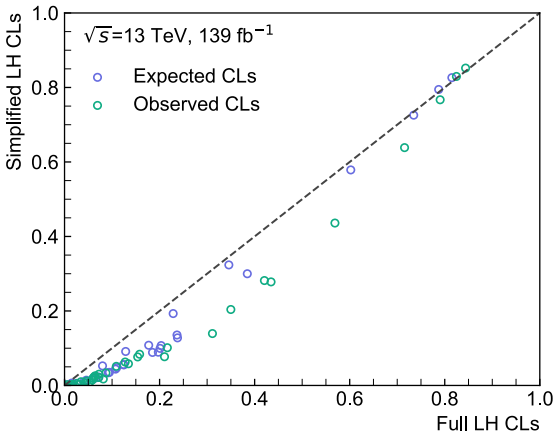

(a) ATLAS direct stau search [275]

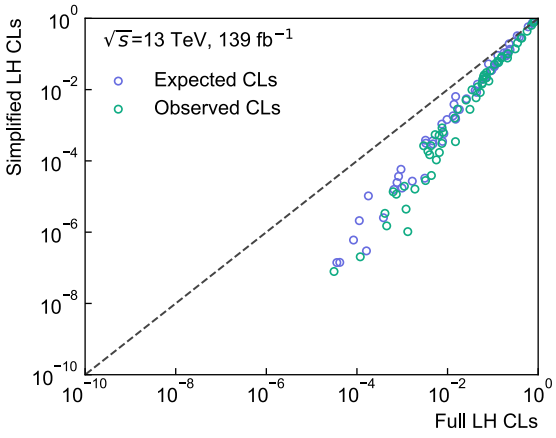

(b) ATLAS direct stau search [275]

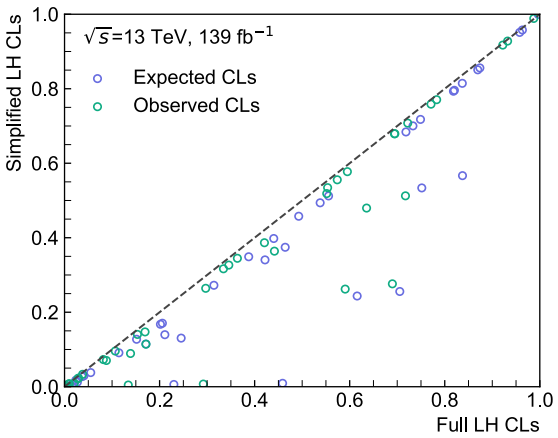

(c) ATLAS 3ℓ search

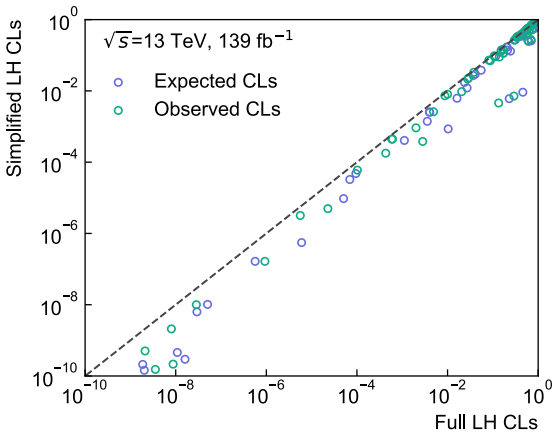

(d) ATLAS 3ℓ search

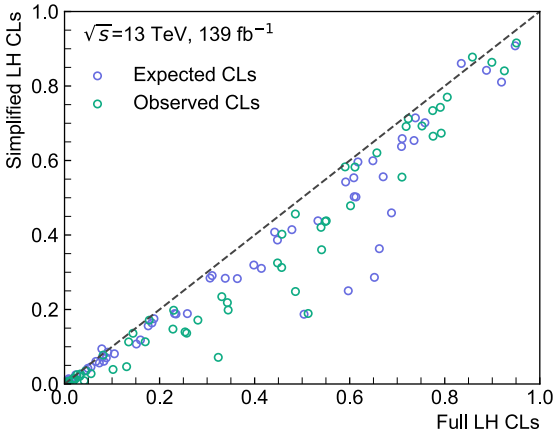

(e) ATLAS compressed search [274]

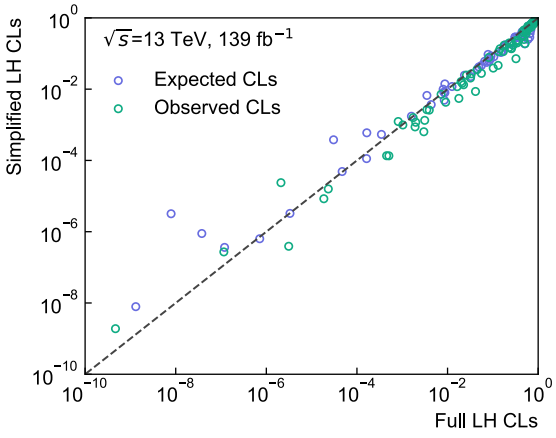

(f) ATLAS compressed search [274]

Figure B.7: Scatter plots comparing the observed and expected CL_s values obtained using the simplified and the full likelihoods for the same set of signal models originally considered in the various ATLAS SUSY searches. Both linear and logarithmic scale representations are shown on the left- and right-hand side, respectively, illustrating the full range of CL_s values. Apart from the scales, both columns show exactly the same results for each row of plots.

Bibliography

[1] ATLAS Collaboration, "Observation of a new particle in the search for the Standard Model Higgs boson with the ATLAS detector at the LHC," *Phys. Lett. B* **716** (2012) 1, arXiv:1207.7214 [hep-ex].

[2] CMS Collaboration, "Observation of a new boson at a mass of 125 GeV with the CMS experiment at the LHC," *Phys. Lett. B* **716** (2012) 30, arXiv:1207.7235 [hep-ex].

[3] I. C. Brock and T. Schorner-Sadenius, *Physics at the terascale*. Wiley, Weinheim, 2011. https://cds.cern.ch/record/1354959.

[4] M. E. Peskin and D. V. Schroeder, *An Introduction to quantum field theory*. Addison-Wesley, Reading, USA, 1995. http://www.slac.stanford.edu/~mpeskin/QFT.html.

[5] S. P. Martin, "A Supersymmetry primer," arXiv:hep-ph/9709356 [hep-ph]. [Adv. Ser. Direct. High Energy Phys.18,1(1998)].

[6] M. Bustamante, L. Cieri, and J. Ellis, "Beyond the Standard Model for Montaneros," in *5th CERN - Latin American School of High-Energy Physics*. 11, 2009. arXiv:0911.4409 [hep-ph].

[7] L. Brown, *The Birth of particle physics*. Cambridge University Press, Cambridge Cambridgeshire New York, 1986.

[8] P. J. Mohr, D. B. Newell, and B. N. Taylor, "CODATA Recommended Values of the Fundamental Physical Constants: 2014," *Rev. Mod. Phys.* **88** no. 3, (2016) 035009, arXiv:1507.07956 [physics.atom-ph].

[9] P. D. Group, "Review of Particle Physics," *Progress of Theoretical and Experimental Physics* **2020** no. 8, (08, 2020) , https://academic.oup.com/ptep/article-pdf/2020/8/083C01/34673722/ptaa104.pdf. https://doi.org/10.1093/ptep/ptaa104. 083C01.

[10] **Super-Kamiokande** Collaboration, Y. Fukuda *et al.*, "Evidence for oscillation of atmospheric neutrinos," *Phys. Rev. Lett.* **81** (1998) 1562–1567, arXiv:hep-ex/9807003 [hep-ex].

[11] Z. Maki, M. Nakagawa, and S. Sakata, "Remarks on the unified model of elementary particles," *Prog. Theor. Phys.* **28** (1962) 870–880. [,34(1962)].

[12] N. Cabibbo, "Unitary symmetry and leptonic decays," *Phys. Rev. Lett.* **10** (Jun, 1963) 531–533. https://link.aps.org/doi/10.1103/PhysRevLett.10.531.

[13] M. Kobayashi and T. Maskawa, "CP Violation in the Renormalizable Theory of Weak Interaction," *Prog. Theor. Phys.* **49** (1973) 652–657.

[14] E. Noether and M. A. Tavel, "Invariant variation problems," arXiv:physics/0503066.

[15] J. C. Ward, "An identity in quantum electrodynamics," *Phys. Rev.* **78** (Apr, 1950) 182–182. https://link.aps.org/doi/10.1103/PhysRev.78.182.

[16] Y. Takahashi, "On the generalized ward identity," *Il Nuovo Cimento (1955-1965)* **6** no. 2, (Aug, 1957) 371–375. https://doi.org/10.1007/BF02832514.

[17] G. 'tHooft, "Renormalization of massless yang-mills fields," *Nuclear Physics B* **33** no. 1, (1971) 173 – 199. http://www.sciencedirect.com/science/article/pii/0550321371903956.

[18] J. Taylor, "Ward identities and charge renormalization of the yang-mills field," *Nuclear Physics B* **33** no. 2, (1971) 436 – 444. http://www.sciencedirect.com/science/article/pii/0550321371902975.

[19] A. A. Slavnov, "Ward identities in gauge theories," *Theoretical and Mathematical Physics* **10** no. 2, (Feb, 1972) 99–104. https://doi.org/10.1007/BF01090719.

[20] C. N. Yang and R. L. Mills, "Conservation of isotopic spin and isotopic gauge invariance," *Phys. Rev.* **96** (Oct, 1954) 191–195. https://link.aps.org/doi/10.1103/PhysRev.96.191.

[21] K. G. Wilson, "Confinement of quarks," *Phys. Rev. D* **10** (Oct, 1974) 2445–2459. https://link.aps.org/doi/10.1103/PhysRevD.10.2445.

[22] T. DeGrand and C. DeTar, *Lattice Methods for Quantum Chromodynamics*. World Scientific, Singapore, 2006. https://cds.cern.ch/record/1055545.

[23] S. L. Glashow, "Partial-symmetries of weak interactions," *Nuclear Physics* **22** no. 4, (1961) 579 – 588. http://www.sciencedirect.com/science/article/pii/0029558261904692.

[24] S. Weinberg, "A model of leptons," *Phys. Rev. Lett.* **19** (Nov, 1967) 1264–1266. https://link.aps.org/doi/10.1103/PhysRevLett.19.1264.

[25] A. Salam and J. C. Ward, "Weak and electromagnetic interactions," *Il Nuovo Cimento (1955-1965)* **11** no. 4, (Feb, 1959) 568–577. https://doi.org/10.1007/BF02726525.

[26] C. S. Wu, E. Ambler, R. W. Hayward, D. D. Hoppes, and R. P. Hudson, "Experimental test of parity conservation in beta decay," *Phys. Rev.* **105** (Feb, 1957) 1413–1415. https://link.aps.org/doi/10.1103/PhysRev.105.1413.

[27] M. Gell-Mann, "The interpretation of the new particles as displaced charge multiplets," *Il Nuovo Cimento (1955-1965)* **4** no. 2, (Apr, 1956) 848–866. https://doi.org/10.1007/BF02748000.

[28] K. Nishijima, "Charge Independence Theory of V Particles*," *Progress of Theoretical Physics* **13** no. 3, (03, 1955) 285–304, https://academic.oup.com/ptp/article-pdf/13/3/285/5425869/13-3-285.pdf. https://doi.org/10.1143/PTP.13.285.

[29] T. Nakano and K. Nishijima, "Charge Independence for V-particles*," *Progress of Theoretical Physics* **10** no. 5, (11, 1953) 581–582, https://academic.oup.com/ptp/article-pdf/10/5/581/5364926/10-5-581.pdf. https://doi.org/10.1143/PTP.10.581.

[30] F. Englert and R. Brout, "Broken symmetry and the mass of gauge vector mesons," *Phys. Rev. Lett.* **13** (Aug, 1964) 321–323. https://link.aps.org/doi/10.1103/PhysRevLett.13.321.

[31] P. W. Higgs, "Broken symmetries and the masses of gauge bosons," *Phys. Rev. Lett.* **13** (Oct, 1964) 508–509. https://link.aps.org/doi/10.1103/PhysRevLett.13.508.

[32] P. W. Higgs, "Spontaneous symmetry breakdown without massless bosons," *Phys. Rev.* **145** (May, 1966) 1156–1163. https://link.aps.org/doi/10.1103/PhysRev.145.1156.

[33] Y. Nambu, "Quasiparticles and Gauge Invariance in the Theory of Superconductivity," *Phys. Rev.* **117** (1960) 648–663. [,132(1960)].

[34] J. Goldstone, "Field Theories with Superconductor Solutions," *Nuovo Cim.* **19** (1961) 154–164.

[35] V. Brdar, A. J. Helmboldt, S. Iwamoto, and K. Schmitz, "Type-I Seesaw as the Common Origin of Neutrino Mass, Baryon Asymmetry, and the Electroweak Scale," *Phys. Rev. D* **100** (2019) 075029, arXiv:1905.12634 [hep-ph].

[36] G. 't Hooft and M. Veltman, "Regularization and renormalization of gauge fields," *Nuclear Physics B* **44** no. 1, (1972) 189 – 213. http://www.sciencedirect.com/science/article/pii/0550321372902799.

[37] F. Zwicky, "Die Rotverschiebung von extragalaktischen Nebeln," *Helv. Phys. Acta* **6** (1933) 110–127. https://cds.cern.ch/record/437297.

[38] V. C. Rubin and W. K. Ford, Jr., "Rotation of the Andromeda Nebula from a Spectroscopic Survey of Emission Regions," *Astrophys. J.* **159** (1970) 379–403.

[39] G. Bertone, D. Hooper, and J. Silk, "Particle dark matter: Evidence, candidates and constraints," *Phys. Rept.* **405** (2005) 279–390, arXiv:hep-ph/0404175.

[40] D. Clowe, M. Bradac, A. H. Gonzalez, M. Markevitch, S. W. Randall, C. Jones, and D. Zaritsky, "A direct empirical proof of the existence of dark matter," *Astrophys. J.* **648** (2006) L109–L113, arXiv:astro-ph/0608407 [astro-ph].

[41] A. Taylor, S. Dye, T. J. Broadhurst, N. Benitez, and E. van Kampen, "Gravitational lens magnification and the mass of abell 1689," *Astrophys. J.* **501** (1998) 539, arXiv:astro-ph/9801158.

[42] C. Bennett *et al.*, "Four year COBE DMR cosmic microwave background observations: Maps and basic results," *Astrophys. J. Lett.* **464** (1996) L1–L4, arXiv:astro-ph/9601067.

[43] G. F. Smoot *et al.*, "Structure in the COBE Differential Microwave Radiometer First-Year Maps," *ApJS* **396** (September, 1992) L1.

[44] **WMAP** Collaboration, "Nine-year Wilkinson Microwave Anisotropy Probe (WMAP) Observations: Final Maps and Results," *ApJS* **208** no. 2, (October, 2013) 20, arXiv:1212.5225 [astro-ph.CO].

[45] **WMAP** Collaboration, "Nine-year Wilkinson Microwave Anisotropy Probe (WMAP) Observations: Cosmological Parameter Results," *ApJS* **208** no. 2, (October, 2013) 19, arXiv:1212.5226 [astro-ph.CO].

[46] **Planck** Collaboration, "Planck 2018 results. I. Overview and the cosmological legacy of Planck," *Astron. Astrophys.* **641** (2020) A1, arXiv:1807.06205 [astro-ph.CO].

[47] A. Liddle, *An introduction to modern cosmology; 3rd ed.* Wiley, Chichester, Mar, 2015. https://cds.cern.ch/record/1976476.

[48] **Planck** Collaboration, "Planck 2018 results. VI. Cosmological parameters," *Astron. Astrophys.* **641** (2020) A6, arXiv:1807.06209 [astro-ph.CO].

[49] H. Georgi and S. L. Glashow, "Unity of all elementary-particle forces," *Phys. Rev. Lett.* **32** (Feb, 1974) 438–441. https://link.aps.org/doi/10.1103/PhysRevLett.32.438.

[50] I. Aitchison, *Supersymmetry in Particle Physics. An Elementary Introduction*. Cambridge University Press, Cambridge, 2007.

[51] **Muon g-2** Collaboration, G. Bennett *et al.*, "Final Report of the Muon E821 Anomalous Magnetic Moment Measurement at BNL," *Phys. Rev. D* **73** (2006) 072003, arXiv:hep-ex/0602035.

[52] H. Baer and X. Tata, *Weak Scale Supersymmetry: From Superfields to Scattering Events*. Cambridge University Press, 2006.

[53] A. Czarnecki and W. J. Marciano, "The Muon anomalous magnetic moment: A Harbinger for 'new physics'," *Phys. Rev. D* **64** (2001) 013014, arXiv:hep-ph/0102122.

[54] J. L. Feng and K. T. Matchev, "Supersymmetry and the anomalous magnetic moment of the muon," *Phys. Rev. Lett.* **86** (2001) 3480–3483, arXiv:hep-ph/0102146.

[55] S. Coleman and J. Mandula, "All possible symmetries of the s matrix," *Phys. Rev.* **159** (Jul, 1967) 1251–1256. https://link.aps.org/doi/10.1103/PhysRev.159.1251.

[56] R. Haag, J. T. Lopuszanski, and M. Sohnius, "All Possible Generators of Supersymmetries of the s Matrix," *Nucl. Phys.* **B88** (1975) 257. [,257(1974)].

[57] J. Wess and B. Zumino, "Supergauge transformations in four dimensions," *Nuclear Physics B* **70** no. 1, (1974) 39 – 50. http://www.sciencedirect.com/science/article/pii/0550321374903551.

[58] H. Georgi and S. L. Glashow, "Gauge theories without anomalies," *Phys. Rev. D* **6** (Jul, 1972) 429–431. https://link.aps.org/doi/10.1103/PhysRevD.6.429.

[59] S. Dimopoulos and D. W. Sutter, "The Supersymmetric flavor problem," *Nucl. Phys. B* **452** (1995) 496–512, arXiv:hep-ph/9504415.

[60] **MEG** Collaboration, T. Mori, "Final Results of the MEG Experiment," *Nuovo Cim. C* **39** no. 4, (2017) 325, arXiv:1606.08168 [hep-ex].

[61] H. P. Nilles, "Supersymmetry, Supergravity and Particle Physics," *Phys. Rept.* **110** (1984) 1–162.

[62] A. Lahanas and D. Nanopoulos, "The road to no-scale supergravity," *Physics Reports* **145** no. 1, (1987) 1 – 139. http://www.sciencedirect.com/science/article/pii/0370157387900342.

[63] J. L. Feng, A. Rajaraman, and F. Takayama, "Superweakly interacting massive particles," *Phys. Rev. Lett.* **91** (2003) 011302, arXiv:hep-ph/0302215.

[64] **Super-Kamiokande** Collaboration, K. Abe *et al.*, "Search for proton decay via $p \to e^+\pi^0$ and $p \to \mu^+\pi^0$ in 0.31 megaton-years exposure of the Super-Kamiokande water Cherenkov detector," *Phys. Rev.* **D95** no. 1, (2017) 012004, arXiv:1610.03597 [hep-ex].

[65] J. R. Ellis, "Beyond the standard model for hill walkers," in *1998 European School of High-Energy Physics*, pp. 133–196. 8, 1998. arXiv:hep-ph/9812235.

[66] J. R. Ellis, J. Hagelin, D. V. Nanopoulos, K. A. Olive, and M. Srednicki, "Supersymmetric Relics from the Big Bang," *Nucl. Phys. B* **238** (1984) 453–476.

[67] D. O. Caldwell, R. M. Eisberg, D. M. Grumm, M. S. Witherell, B. Sadoulet, F. S. Goulding, and A. R. Smith, "Laboratory limits on galactic cold dark matter," *Phys. Rev. Lett.* **61** (Aug, 1988) 510–513. https://link.aps.org/doi/10.1103/PhysRevLett.61.510.

[68] M. Mori, M. M. Nojiri, K. S. Hirata, K. Kihara, Y. Oyama, A. Suzuki, K. Takahashi, M. Yamada, H. Takei, M. Koga, K. Miyano, H. Miyata, Y. Fukuda, T. Hayakawa, K. Inoue, T. Ishida, T. Kajita, Y. Koshio, M. Nakahata, K. Nakamura, A. Sakai, N. Sato, M. Shiozawa, J. Suzuki, Y. Suzuki, Y. Totsuka, M. Koshiba, K. Nishijima, T. Kajimura, T. Suda, A. T. Suzuki, T. Hara, Y. Nagashima, M. Takita, H. Yokoyama, A. Yoshimoto, K. Kaneyuki, Y. Takeuchi, T. Tanimori, S. Tasaka, and K. Nishikawa, "Search for neutralino dark matter heavier than the w boson at kamiokande," *Phys. Rev. D* **48** (Dec, 1993) 5505–5518. https://link.aps.org/doi/10.1103/PhysRevD.48.5505.

[69] **CDMS** Collaboration, D. S. Akerib *et al.*, "Exclusion limits on the WIMP-nucleon cross section from the first run of the Cryogenic Dark Matter Search in the Soudan Underground Laboratory," *Phys. Rev. D* **72** (2005) 052009, arXiv:astro-ph/0507190.

[70] A. Djouadi, J.-L. Kneur, and G. Moultaka, "SuSpect: A Fortran code for the supersymmetric and Higgs particle spectrum in the MSSM," *Comput. Phys. Commun.* **176** (2007) 426–455, arXiv:hep-ph/0211331.

[71] C. F. Berger, J. S. Gainer, J. L. Hewett, and T. G. Rizzo, "Supersymmetry without prejudice," *Journal of High Energy Physics* **2009** no. 02, (Feb, 2009) 023–023. http://dx.doi.org/10.1088/1126-6708/2009/02/023.

[72] J. Alwall, P. Schuster, and N. Toro, "Simplified Models for a First Characterization of New Physics at the LHC," *Phys. Rev.* **D79** (2009) 075020, arXiv:0810.3921 [hep-ph].

[73] **LHC New Physics Working Group** Collaboration, D. Alves, "Simplified Models for LHC New Physics Searches," *J. Phys.* **G39** (2012) 105005, arXiv:1105.2838 [hep-ph].

[74] D. S. Alves, E. Izaguirre, and J. G. Wacker, "Where the Sidewalk Ends: Jets and Missing Energy Search Strategies for the 7 TeV LHC," *JHEP* **10** (2011) 012, arXiv:1102.5338 [hep-ph].

[75] F. Ambrogi, S. Kraml, S. Kulkarni, U. Laa, A. Lessa, and W. Waltenberger, "On the coverage of the pMSSM by simplified model results," *Eur. Phys. J. C* **78** no. 3, (2018) 215, arXiv:1707.09036 [hep-ph].

[76] O. Buchmueller and J. Marrouche, "Universal mass limits on gluino and third-generation squarks in the context of Natural-like SUSY spectra," *Int. J. Mod. Phys. A* **29** no. 06, (2014) 1450032, arXiv:1304.2185 [hep-ph].

[77] **ATLAS** Collaboration, M. Aaboud *et al.*, "Dark matter interpretations of ATLAS searches for the electroweak production of supersymmetric particles in $\sqrt{s} = 8$ TeV proton-proton collisions," *JHEP* **09** (2016) 175, arXiv:1608.00872 [hep-ex].

[78] **ATLAS** Collaboration, "Summary of the ATLAS experiment's sensitivity to supersymmetry after LHC Run 1 — interpreted in the phenomenological MSSM," *JHEP* **10** (2015) 134, arXiv:1508.06608 [hep-ex].

[79] **ATLAS** Collaboration, "Mass reach of the atlas searches for supersymmetry." https://atlas.web.cern.ch/Atlas/GROUPS/PHYSICS/PUBNOTES/ATL-PHYS-PUB-2020-020/fig_23.png, 2020.

[80] **CMS** Collaboration, "Summary plot moriond 2017." https://twiki.cern.ch/twiki/pub/CMSPublic/SUSYSummary2017/Moriond2017_BarPlot.pdf, 2017.

[81] L. S. W. Group, "Notes lepsusywg/02-04.1 and lepsusywg/01-03.1." http://lepsusy.web.cern.ch/lepsusy/, 2004. Accessed: 2021-02-11.

[82] **ATLAS** Collaboration, G. Aad *et al.*, "Observation of a new particle in the search for the Standard Model Higgs boson with the ATLAS detector at the LHC," *Phys. Lett. B* **716** (2012) 1–29, arXiv:1207.7214 [hep-ex].

[83] **CMS** Collaboration, S. Chatrchyan *et al.*, "Observation of a New Boson at a Mass of 125 GeV with the CMS Experiment at the LHC," *Phys. Lett. B* **716** (2012) 30–61, arXiv:1207.7235 [hep-ex].

[84] CERN, "About cern." https://home.cern/about. Accessed: 2021-01-21.

[85] CERN, "CERN Annual report 2019," tech. rep., CERN, Geneva, 2020. https://cds.cern.ch/record/2723123.

[86] O. S. Bruning, P. Collier, P. Lebrun, S. Myers, R. Ostojic, J. Poole, and P. Proudlock, *LHC Design Report*. CERN Yellow Reports: Monographs. CERN, Geneva, 2004. https://cds.cern.ch/record/782076.

[87] M. Blewett and N. Vogt-Nilsen, "Proceedings of the 8th international conference on high-energy accelerators, cern 1971. conference held at geneva, 20–24 september 1971.," tech. rep., 1971, 1971.

[88] L. R. Evans and P. Bryant, "LHC Machine," *JINST* **3** (2008) S08001. 164 p. http://cds.cern.ch/record/1129806. This report is an abridged version of the LHC Design Report (CERN-2004-003).

[89] R. Scrivens, M. Kronberger, D. Küchler, J. Lettry, C. Mastrostefano, O. Midttun, M. O'Neil, H. Pereira, and C. Schmitzer, "Overview of the status and developments on primary ion sources at CERN*,". https://cds.cern.ch/record/1382102.

[90] M. Vretenar, J. Vollaire, R. Scrivens, C. Rossi, F. Roncarolo, S. Ramberger, U. Raich, B. Puccio, D. Nisbet, R. Mompo, S. Mathot, C. Martin, L. A. Lopez-Hernandez, A. Lombardi, J. Lettry, J. B. Lallement, I. Kozsar, J. Hansen, F. Gerigk, A. Funken, J. F. Fuchs, N. Dos Santos, M. Calviani, M. Buzio, O. Brunner, Y. Body, P. Baudrenghien, J. Bauche, and T. Zickler, *Linac4 design report*, vol. 6 of *CERN Yellow Reports: Monographs*. CERN, Geneva, 2020. https://cds.cern.ch/record/2736208.

[91] E. Mobs, "The CERN accelerator complex - 2019. Complexe des accélérateurs du CERN - 2019,". https://cds.cern.ch/record/2684277. General Photo.

[92] **ATLAS** Collaboration, "The ATLAS Experiment at the CERN Large Hadron Collider," *JINST* **3** (2008) S08003.

[93] **CMS** Collaboration, S. Chatrchyan *et al.*, "The CMS Experiment at the CERN LHC," *JINST* **3** (2008) S08004.

[94] **ALICE** Collaboration, K. Aamodt *et al.*, "The ALICE experiment at the CERN LHC," *JINST* **3** (2008) S08002.

[95] **LHCb** Collaboration, J. Alves, A.Augusto *et al.*, "The LHCb Detector at the LHC," *JINST* **3** (2008) S08005.

[96] **TOTEM** Collaboration, G. Anelli *et al.*, "The TOTEM experiment at the CERN Large Hadron Collider," *JINST* **3** (2008) S08007.

[97] **LHCf** Collaboration, O. Adriani *et al.*, "Technical design report of the LHCf experiment: Measurement of photons and neutral pions in the very forward region of LHC,".

[98] **MoEDAL** Collaboration, J. Pinfold *et al.*, "Technical Design Report of the MoEDAL Experiment,".

[99] **ATLAS** Collaboration, "ATLAS Public Results - Luminosity Public Results Run 2,". https://twiki.cern.ch/twiki/bin/view/AtlasPublic/LuminosityPublicResultsRun2. Accessed: 2021-01-17.

[100] **ATLAS** Collaboration, Z. Marshall, "Simulation of Pile-up in the ATLAS Experiment," *J. Phys. Conf. Ser.* **513** (2014) 022024.

[101] "First beam in the LHC - accelerating science,". https://home.cern/news/news/accelerators/record-luminosity-well-done-lhc. Accessed: 2021-01-10.

[102] **ATLAS Collaboration** Collaboration, "Luminosity determination in pp collisions at $\sqrt{s} = 13$ TeV using the ATLAS detector at the LHC," Tech. Rep. ATLAS-CONF-2019-021, CERN, Geneva, Jun, 2019. https://cds.cern.ch/record/2677054.

[103] **ATLAS** Collaboration, M. Aaboud *et al.*, "Luminosity determination in pp collisions at $\sqrt{s} = 8$ TeV using the ATLAS detector at the LHC," *Eur. Phys. J. C* **76** no. 12, (2016) 653, arXiv:1608.03953 [hep-ex].

[104] G. Avoni, M. Bruschi, G. Cabras, D. Caforio, N. Dehghanian, A. Floderus, B. Giacobbe, F. Giannuzzi, F. Giorgi, P. Grafström, V. Hedberg, F. L. Manghi, S. Meneghini, J. Pinfold, E. Richards, C. Sbarra, N. S. Cesari, A. Sbrizzi, R. Soluk, G. Ucchielli, S. Valentinetti, O. Viazlo, M. Villa, C. Vittori, R. Vuillermet, and A. Zoccoli, "The new LUCID-2 detector for luminosity measurement and monitoring in ATLAS," *Journal of Instrumentation* **13** no. 07, (Jul, 2018) P07017–P07017. https://doi.org/10.1088/1748-0221/13/07/p07017.

[105] S. van der Meer, "Calibration of the effective beam height in the ISR," Tech. Rep. CERN-ISR-PO-68-31. ISR-PO-68-31, CERN, Geneva, 1968. https://cds.cern.ch/record/296752.

[106] P. Grafström and W. Kozanecki, "Luminosity determination at proton colliders," *Progress in Particle and Nuclear Physics* **81** (2015) 97 – 148. http://www.sciencedirect.com/science/article/pii/S0146641014000878.

[107] "New schedule for CERN's accelerators and experiments,". https://home.cern/news/press-release/cern/first-beam-lhc-accelerating-science. Accessed: 2021-01-10.

[108] **ATLAS** Collaboration, G. Aad *et al.*, "Luminosity Determination in *pp* Collisions at $\sqrt{s} = 7$ TeV Using the ATLAS Detector at the LHC," *Eur. Phys. J. C* **71** (2011) 1630, arXiv:1101.2185 [hep-ex].

[109] **ATLAS Collaboration** Collaboration, G. Aad *et al.*, "Improved luminosity determination in pp collisions at $\sqrt{s} = 7$ TeV using the ATLAS detector at the LHC. Improved luminosity determination in pp collisions at sqrt(s) = 7 TeV using the ATLAS detector at the LHC," *Eur. Phys. J. C* **73** no. CERN-PH-EP-2013-026. CERN-PH-EP-2013-026, (Feb, 2013) 2518. 27 p. https://cds.cern.ch/record/1517411. Comments: 26 pages plus author list (39 pages total), 17 figures, 9 tables, submitted to EPJC, All figures are available at <a href=.

[110] "Record luminosity: well done LHC,". https://home.cern/news/news/accelerators/new-schedule-cerns-accelerators-and-experiments. Accessed: 2021-01-10.

[111] A. G., B. A. I., B. O., F. P., L. M., R. L., and T. L., *High-Luminosity Large Hadron Collider (HL-LHC): Technical Design Report V. 0.1*. CERN Yellow Reports: Monographs. CERN, Geneva, 2017. https://cds.cern.ch/record/2284929.

[112] J. Pequenao, "Computer generated image of the whole ATLAS detector." Mar, 2008.

[113] **ATLAS** Collaboration, "ATLAS: Detector and physics performance technical design report. Volume 1,".

[114] J. Pequenao, "Computer generated image of the ATLAS inner detector." Mar, 2008.

[115] **ATLAS Collaboration** Collaboration, K. Potamianos, "The upgraded Pixel detector and the commissioning of the Inner Detector tracking of the ATLAS experiment for Run-2 at the Large Hadron Collider," Tech. Rep. ATL-PHYS-PROC-2016-104, CERN, Geneva, Aug, 2016. https://cds.cern.ch/record/2209070. 15 pages, EPS-HEP 2015 Proceedings.

[116] **ATLAS IBL** Collaboration, B. Abbott *et al.*, "Production and Integration of the ATLAS Insertable B-Layer," *JINST* **13** no. 05, (2018) T05008, arXiv:1803.00844 [physics.ins-det].

[117] **ATLAS** Collaboration, "ATLAS Insertable B-Layer Technical Design Report," Tech. Rep. CERN-LHCC-2010-013. ATLAS-TDR-19, Sep, 2010. http://cds.cern.ch/record/1291633.

[118] **ATLAS** Collaboration, G. Aad *et al.*, "ATLAS b-jet identification performance and efficiency measurement with $t\bar{t}$ events in pp collisions at $\sqrt{s} = 13$ TeV," *Eur. Phys. J. C* **79** no. 11, (2019) 970, arXiv:1907.05120 [hep-ex].

[119] ATLAS Collaboration, "Particle Identification Performance of the ATLAS Transition Radiation Tracker." ATLAS-CONF-2011-128, 2011. https://cds.cern.ch/record/1383793.

[120] J. Pequenao, "Computer Generated image of the ATLAS calorimeter." Mar, 2008.

[121] J. Pequenao, "Computer generated image of the ATLAS Muons subsystem." Mar, 2008.

[122] S. Lee, M. Livan, and R. Wigmans, "Dual-Readout Calorimetry," *Rev. Mod. Phys.* **90** no. arXiv:1712.05494. 2, (Dec, 2017) 025002. 40 p. https://cds.cern.ch/record/2637852. 44 pages, 53 figures, accepted for publication in Review of Modern Physics.

[123] M. Leite, "Performance of the ATLAS Zero Degree Calorimeter," Tech. Rep. ATL-FWD-PROC-2013-001, CERN, Geneva, Nov, 2013. https://cds.cern.ch/record/1628749.

[124] S. Abdel Khalek *et al.*, "The ALFA Roman Pot Detectors of ATLAS," *JINST* **11** no. 11, (2016) P11013, arXiv:1609.00249 [physics.ins-det].

[125] U. Amaldi, G. Cocconi, A. Diddens, R. Dobinson, J. Dorenbosch, W. Duinker, D. Gustavson, J. Meyer, K. Potter, A. Wetherell, A. Baroncelli, and C. Bosio, "The real part of the forward proton proton scattering amplitude measured at the cern intersecting storage rings," *Physics Letters B* **66** no. 4, (1977) 390 – 394. http://www.sciencedirect.com/science/article/pii/0370269377900223.

[126] L. Adamczyk, E. Banaś, A. Brandt, M. Bruschi, S. Grinstein, J. Lange, M. Rijssenbeek, P. Sicho, R. Staszewski, T. Sykora, M. Trzebiński, J. Chwastowski, and K. Korcyl, "Technical Design Report for the ATLAS Forward Proton Detector," Tech. Rep. CERN-LHCC-2015-009. ATLAS-TDR-024, May, 2015. https://cds.cern.ch/record/2017378.

[127] **ATLAS** Collaboration, A. R. Martínez, "The Run-2 ATLAS Trigger System," *J. Phys. Conf. Ser.* **762** no. 1, (2016) 012003.

[128] **ATLAS Collaboration** Collaboration, *ATLAS level-1 trigger: Technical Design Report*. Technical Design Report ATLAS. CERN, Geneva, 1998. https://cds.cern.ch/record/381429.

[129] **ATLAS** Collaboration, G. Aad *et al.*, "Operation of the ATLAS trigger system in Run 2," *JINST* **15** no. 10, (2020) P10004, arXiv:2007.12539 [physics.ins-det].

[130] **ATLAS Collaboration** Collaboration, P. Jenni, M. Nessi, M. Nordberg, and K. Smith, *ATLAS high-level trigger, data-acquisition and controls: Technical Design Report*. Technical Design Report ATLAS. CERN, Geneva, 2003. https://cds.cern.ch/record/616089.

[131] **ATLAS** Collaboration, G. Aad *et al.*, "The ATLAS Simulation Infrastructure," *Eur. Phys. J. C* **70** (2010) 823–874, arXiv:1005.4568 [physics.ins-det].

[132] T. Gleisberg, S. Hoeche, F. Krauss, M. Schonherr, S. Schumann, F. Siegert, and J. Winter, "Event generation with SHERPA 1.1," *JHEP* **02** (2009) 007, arXiv:0811.4622 [hep-ph].

[133] A. Buckley *et al.*, "General-purpose event generators for LHC physics," *Phys. Rept.* **504** (2011) 145–233, arXiv:1101.2599 [hep-ph].

[134] V. N. Gribov and L. N. Lipatov, "Deep inelastic e p scattering in perturbation theory," *Sov. J. Nucl. Phys.* **15** (1972) 438–450.

[135] J. Blumlein, T. Doyle, F. Hautmann, M. Klein, and A. Vogt, "Structure functions in deep inelastic scattering at HERA," in *Workshop on Future Physics at HERA (To be followed by meetings 7-9 Feb and 30-31 May 1996 at DESY)*. 9, 1996. arXiv:hep-ph/9609425.

[136] A. Buckley, J. Ferrando, S. Lloyd, K. Nordström, B. Page, M. Rüfenacht, M. Schönherr, and G. Watt, "LHAPDF6: parton density access in the LHC precision era," *Eur. Phys. J. C* **75** (2015) 132, arXiv:1412.7420 [hep-ph].

[137] M. Bengtsson and T. Sjostrand, "Coherent Parton Showers Versus Matrix Elements: Implications of PETRA - PEP Data," *Phys. Lett. B* **185** (1987) 435.

[138] S. Catani, F. Krauss, R. Kuhn, and B. R. Webber, "QCD matrix elements + parton showers," *JHEP* **11** (2001) 063, arXiv:hep-ph/0109231.

[139] L. Lonnblad, "Correcting the color dipole cascade model with fixed order matrix elements," *JHEP* **05** (2002) 046, arXiv:hep-ph/0112284.

[140] B. Andersson, G. Gustafson, G. Ingelman, and T. Sjostrand, "Parton Fragmentation and String Dynamics," *Phys. Rept.* **97** (1983) 31–145.

[141] B. Andersson, *The Lund Model*. Cambridge Monographs on Particle Physics, Nuclear Physics and Cosmology. Cambridge University Press, 1998.

[142] D. Amati and G. Veneziano, "Preconfinement as a Property of Perturbative QCD," *Phys. Lett. B* **83** (1979) 87–92.

[143] D. Yennie, S. Frautschi, and H. Suura, "The infrared divergence phenomena and high-energy processes," *Annals of Physics* **13** no. 3, (1961) 379–452. https://www.sciencedirect.com/science/article/pii/0003491661901518.

[144] M. Dobbs and J. B. Hansen, "The HepMC C++ Monte Carlo event record for High Energy Physics," *Comput. Phys. Commun.* **134** (2001) 41–46.

[145] **GEANT4** Collaboration, S. Agostinelli *et al.*, "GEANT4: A Simulation toolkit," *Nucl. Instrum. Meth.* **A506** (2003) 250–303.

[146] **ATLAS Collaboration** Collaboration, "The new Fast Calorimeter Simulation in ATLAS," Tech. Rep. ATL-SOFT-PUB-2018-002, CERN, Geneva, Jul, 2018. https://cds.cern.ch/record/2630434.

[147] K. Cranmer, "Practical Statistics for the LHC," in *2011 European School of High-Energy Physics*, pp. 267–308. 2014. arXiv:1503.07622 [physics.data-an].

[148] G. Cowan, K. Cranmer, E. Gross, and O. Vitells, "Asymptotic formulae for likelihood-based tests of new physics," *Eur. Phys. J.* **C71** (2011) 1554, arXiv:1007.1727 [physics.data-an]. [Erratum: Eur. Phys. J.C73,2501(2013)].

[149] ATLAS Collaboration, "Reproduction searches for new physics with the ATLAS experiment through publication of full statistical likelihoods." ATL-PHYS-PUB-2019-029, 2019. https://cds.cern.ch/record/2684863.

[150] **ROOT Collaboration** Collaboration, K. Cranmer, G. Lewis, L. Moneta, A. Shibata, and W. Verkerke, "HistFactory: A tool for creating statistical models for use with RooFit and RooStats," Tech. Rep. CERN-OPEN-2012-016, New York U., New York, Jan, 2012. https://cds.cern.ch/record/1456844.

[151] W. Verkerke and D. P. Kirkby, "The RooFit toolkit for data modeling," *eConf* **C0303241** (2003) MOLT007, arXiv:physics/0306116 [physics]. [,186(2003)].

[152] L. Moneta, K. Belasco, K. S. Cranmer, S. Kreiss, A. Lazzaro, D. Piparo, G. Schott, W. Verkerke, and M. Wolf, "The RooStats Project," *PoS* **ACAT2010** (2010) 057, arXiv:1009.1003 [physics.data-an].

[153] F. James and M. Roos, "MINUIT: a system for function minimization and analysis of the parameter errors and corrections," *Comput. Phys. Commun.* **10** no. CERN-DD-75-20, (Jul, 1975) 343–367. 38 p. https://cds.cern.ch/record/310399.

[154] R. Brun and F. Rademakers, "ROOT: An object oriented data analysis framework," *Nucl. Instrum. Meth.* **A389** (1997) 81–86.

[155] I. Antcheva *et al.*, "Root — a c++ framework for petabyte data storage, statistical analysis and visualization," *Computer Physics Communications* **182** no. 6, (2011) 1384 – 1385. http://www.sciencedirect.com/science/article/pii/S0010465511000701.

[156] M. Baak, G. J. Besjes, D. Côte, A. Koutsman, J. Lorenz, and D. Short, "HistFitter software framework for statistical data analysis," *Eur. Phys. J.* **C75** (2015) 153, arXiv:1410.1280 [hep-ex].

[157] L. Heinrich, M. Feickert, G. Stark, and K. Cranmer, "pyhf: pure-python implementation of histfactory statistical models," *Journal of Open Source Software* **6** no. 58, (2021) 2823. https://doi.org/10.21105/joss.02823.

[158] L. Heinrich, M. Feickert, and G. Stark, "pyhf: v0.6.0." https://github.com/scikit-hep/pyhf.

[159] C. R. Harris, K. J. Millman, S. J. van der Walt, R. Gommers, P. Virtanen, D. Cournapeau, E. Wieser, J. Taylor, S. Berg, N. J. Smith, R. Kern, M. Picus, S. Hoyer, M. H. van Kerkwijk, M. Brett, A. Haldane, J. F. del R'ıo, M. Wiebe, P. Peterson, P. G'erard-Marchant, K. Sheppard, T. Reddy, W. Weckesser, H. Abbasi, C. Gohlke, and T. E. Oliphant, "Array programming with NumPy," *Nature* **585** no. 7825, (Sept., 2020) 357–362. https://doi.org/10.1038/s41586-020-2649-2.

[160] A. Paszke, S. Gross, F. Massa, A. Lerer, J. Bradbury, G. Chanan, T. Killeen, Z. Lin, N. Gimelshein, L. Antiga, A. Desmaison, A. Kopf, E. Yang, Z. DeVito, M. Raison, A. Tejani, S. Chilamkurthy, B. Steiner, L. Fang, J. Bai, and S. Chintala, "Pytorch: An imperative style, high-performance deep learning library," in *Advances in Neural Information Processing Systems 32*, H. Wallach, H. Larochelle, A. Beygelzimer, F. d'Alché-Buc, E. Fox, and R. Garnett, eds., pp. 8024–8035. Curran Associates, Inc., 2019. http://papers.neurips.cc/paper/9015-pytorch-an-imperative-style-high-performance-deep-learning-library.pdf.

[161] M. Abadi, A. Agarwal, P. Barham, E. Brevdo, Z. Chen, C. Citro, G. S. Corrado, A. Davis, J. Dean, M. Devin, S. Ghemawat, I. Goodfellow, A. Harp, G. Irving, M. Isard, Y. Jia, R. Jozefowicz, L. Kaiser, M. Kudlur, J. Levenberg, D. Mané, R. Monga, S. Moore, D. Murray, C. Olah, M. Schuster, J. Shlens, B. Steiner, I. Sutskever, K. Talwar, P. Tucker, V. Vanhoucke, V. Vasudevan, F. Viégas, O. Vinyals, P. Warden, M. Wattenberg, M. Wicke, Y. Yu, and X. Zheng, "TensorFlow: Large-scale machine learning on heterogeneous systems," 2015. https://www.tensorflow.org/. Software available from tensorflow.org.

[162] J. Bradbury, R. Frostig, P. Hawkins, M. J. Johnson, C. Leary, D. Maclaurin, and S. Wanderman-Milne, "JAX: composable transformations of Python+NumPy programs," 2018. http://github.com/google/jax.

[163] S. S. Wilks, "The large-sample distribution of the likelihood ratio for testing composite hypotheses," *Ann. Math. Statist.* **9** no. 1, (03, 1938) 60–62. https://doi.org/10.1214/aoms/1177732360.

[164] A. Wald, "Tests of statistical hypotheses concerning several parameters when the number of observations is large," *Transactions of the American Mathematical Society* **54** no. 3, (1943) 426–482. https://doi.org/10.1090/S0002-9947-1943-0012401-3.

[165] G. Cowan, "Statistics for Searches at the LHC," in *69th Scottish Universities Summer School in Physics: LHC Physics*, pp. 321–355. 7, 2013. arXiv:1307.2487 [hep-ex].

[166] A. L. Read, "Presentation of search results: the CL_S technique," *J. Phys. G* **28** (2002) 2693.

[167] R. D. Cousins, J. T. Linnemann, and J. Tucker, "Evaluation of three methods for calculating statistical significance when incorporating a systematic uncertainty into a test of the background-only hypothesis for a Poisson process," *Nucl. Instrum. Meth. A* **595** no. 2, (2008) 480, arXiv:physics/0702156 [physics.data-an].

[168] K. CRANMER, "Statistical challenges for searches for new physics at the lhc," *Statistical Problems in Particle Physics, Astrophysics and Cosmology* (May, 2006) . http://dx.doi.org/10.1142/9781860948985_0026.

[169] ATLAS Collaboration, "Search for direct pair production of a chargino and a neutralino decaying to the 125 GeV Higgs boson in $\sqrt{s} = 8$ TeV pp collisions with the ATLAS detector," *Eur. Phys. J. C* **75** (2015) 208, arXiv:1501.07110 [hep-ex].

[170] ATLAS Collaboration, "Search for chargino and neutralino production in final states with a Higgs boson and missing transverse momentum at $\sqrt{s} = 13$ TeV with the ATLAS detector," *Phys. Rev. D* **100** (2019) 012006, arXiv:1812.09432 [hep-ex].

[171] CMS Collaboration, "Search for electroweak production of charginos and neutralinos in WH events in proton–proton collisions at $\sqrt{s} = 13$ TeV," *JHEP* **11** (2017) 029, arXiv:1706.09933 [hep-ex].

[172] ATLAS Collaboration, "Search for direct production of electroweakinos in final states with one lepton, missing transverse momentum and a Higgs boson decaying into two b-jets in pp collisions at $\sqrt{s} = 13$ TeV with the ATLAS detector," *Eur. Phys. J. C* **80** (2020) 691, arXiv:1909.09226 [hep-ex].

[173] ATLAS Collaboration, "Improvements in $t\bar{t}$ modelling using NLO+PS Monte Carlo generators for Run 2." ATL-PHYS-PUB-2018-009, 2018. https://cds.cern.ch/record/2630327.

[174] ATLAS Collaboration, "Modelling of the $t\bar{t}H$ and $t\bar{t}V(V = W, Z)$ processes for $\sqrt{s} = 13$ TeV ATLAS analyses." ATL-PHYS-PUB-2016-005, 2016. https://cds.cern.ch/record/2120826.

[175] ATLAS Collaboration, "ATLAS simulation of boson plus jets processes in Run 2." ATL-PHYS-PUB-2017-006, 2017. https://cds.cern.ch/record/2261937.

[176] ATLAS Collaboration, "Multi-Boson Simulation for 13 TeV ATLAS Analyses." ATL-PHYS-PUB-2017-005, 2017. https://cds.cern.ch/record/2261933.

[177] J. Alwall, R. Frederix, S. Frixione, V. Hirschi, F. Maltoni, O. Mattelaer, H. S. Shao, T. Stelzer, P. Torrielli, and M. Zaro, "The automated computation of tree-level and next-to-leading order differential cross sections, and their matching to parton shower simulations," *JHEP* **07** (2014) 079, arXiv:1405.0301 [hep-ph].

[178] R. Frederix and S. Frixione, "Merging meets matching in MC@NLO," *JHEP* **12** (2012) 061, arXiv:1209.6215 [hep-ph].

[179] T. Sjöstrand, S. Ask, J. R. Christiansen, R. Corke, N. Desai, P. Ilten, S. Mrenna, S. Prestel, C. O. Rasmussen, and P. Z. Skands, "An Introduction to PYTHIA 8.2," *Comput. Phys. Commun.* **191** (2015) 159–177, arXiv:1410.3012 [hep-ph].

[180] L. Lönnblad and S. Prestel, "Matching tree-level matrix elements with interleaved showers," *JHEP* **03** (2012) 019, arXiv:1109.4829 [hep-ph].

[181] R. D. Ball *et al.*, "Parton distributions with LHC data," *Nucl. Phys. B* **867** (2013) 244, arXiv:1207.1303 [hep-ph].

[182] ATLAS Collaboration, "ATLAS Pythia 8 tunes to 7 TeV data." ATL-PHYS-PUB-2014-021, 2014. https://cds.cern.ch/record/1966419.

[183] D. J. Lange, "The EvtGen particle decay simulation package," *Nucl. Instrum. Meth. A* **462** (2001) 152.

[184] ATLAS Collaboration, "The Pythia 8 A3 tune description of ATLAS minimum bias and inelastic measurements incorporating the Donnachie–Landshoff diffractive model." ATL-PHYS-PUB-2016-017, 2016. https://cds.cern.ch/record/2206965.

[185] B. Fuks, M. Klasen, D. R. Lamprea, and M. Rothering, "Precision predictions for electroweak superpartner production at hadron colliders with RESUMMINO," *Eur. Phys. J. C* **73** (2013) 2480, arXiv:1304.0790 [hep-ph].

[186] J. Fiaschi and M. Klasen, "Neutralino-chargino pair production at NLO+NLL with resummation-improved parton density functions for LHC Run II," *Phys. Rev. D* **98** no. 5, (2018) 055014, arXiv:1805.11322 [hep-ph].

[187] B. Fuks, M. Klasen, D. R. Lamprea, and M. Rothering, "Gaugino production in proton-proton collisions at a center-of-mass energy of 8 TeV," *JHEP* **10** (2012) 081, arXiv:1207.2159 [hep-ph].

[188] S. Alioli, P. Nason, C. Oleari, and E. Re, "A general framework for implementing NLO calculations in shower Monte Carlo programs: the POWHEG BOX," *JHEP* **06** (2010) 043, arXiv:1002.2581 [hep-ph].

[189] S. Frixione, P. Nason, and G. Ridolfi, "A Positive-weight next-to-leading-order Monte Carlo for heavy flavour hadroproduction," *JHEP* **09** (2007) 126, arXiv:0707.3088 [hep-ph].

[190] P. Nason, "A New method for combining NLO QCD with shower Monte Carlo algorithms," *JHEP* **11** (2004) 040, arXiv:hep-ph/0409146.

[191] E. Bothmann *et al.*, "Event generation with Sherpa 2.2," *SciPost Phys.* **7** no. 3, (2019) 034, arXiv:1905.09127 [hep-ph].

[192] S. Höche, F. Krauss, S. Schumann, and F. Siegert, "QCD matrix elements and truncated showers," *JHEP* **05** (2009) 053, arXiv:0903.1219 [hep-ph].

[193] S. Höche, F. Krauss, M. Schönherr, and F. Siegert, "QCD matrix elements + parton showers. The NLO case," *JHEP* **04** (2013) 027, arXiv:1207.5030 [hep-ph].

[194] **NNPDF** Collaboration, R. D. Ball *et al.*, "Parton distributions for the LHC run II," *JHEP* **04** (2015) 040, arXiv:1410.8849 [hep-ph].

[195] ATLAS Collaboration, "Example ATLAS tunes of Pythia8, Pythia6 and Powheg to an observable sensitive to Z boson transverse momentum." ATL-PHYS-PUB-2013-017, 2013. https://cds.cern.ch/record/1629317.

[196] M. Czakon and A. Mitov, "Top++: A program for the calculation of the top-pair cross-section at hadron colliders," *Comput. Phys. Commun.* **185** (2014) 2930, arXiv:1112.5675 [hep-ph].

[197] M. Cacciari, M. Czakon, M. Mangano, A. Mitov, and P. Nason, "Top-pair production at hadron colliders with next-to-next-to-leading logarithmic soft-gluon resummation," *Phys. Lett. B* **710** (2012) 612–622, arXiv:1111.5869 [hep-ph].

[198] P. Kant, O. M. Kind, T. Kintscher, T. Lohse, T. Martini, S. Mölbitz, P. Rieck, and P. Uwer, "HatHor for single top-quark production: Updated predictions and uncertainty estimates for single top-quark production in hadronic collisions," *Comput. Phys. Commun.* **191** (2015) 74–89, arXiv:1406.4403 [hep-ph].

[199] N. Kidonakis, "Two-loop soft anomalous dimensions for single top quark associated production with a W^- or H^-," *Phys. Rev. D* **82** (2010) 054018, arXiv:1005.4451 [hep-ph].

[200] J. M. Campbell and R. K. Ellis, "$t\bar{t}W^{+-}$ production and decay at NLO," *JHEP* **07** (2012) 052, arXiv:1204.5678 [hep-ph].

[201] A. Lazopoulos, T. McElmurry, K. Melnikov, and F. Petriello, "Next-to-leading order QCD corrections to $t\bar{t}Z$ production at the LHC," *Phys. Lett. B* **666** (2008) 62–65, arXiv:0804.2220 [hep-ph].

[202] R. Gavin, Y. Li, F. Petriello, and S. Quackenbush, "FEWZ 2.0: A code for hadronic Z production at next-to-next-to-leading order," arXiv:1011.3540 [hep-ph].

[203] **LHC Higgs Cross Section Working Group** Collaboration, D. de Florian *et al.*, "Handbook of LHC Higgs Cross Sections: 4. Deciphering the Nature of the Higgs Sector," arXiv:1610.07922 [hep-ph].

[204] ATLAS Collaboration, "Performance of the ATLAS track reconstruction algorithms in dense environments in LHC Run 2," *Eur. Phys. J. C* **77** (2017) 673, arXiv:1704.07983 [hep-ex].

[205] R. Frühwirth, "Application of Kalman filtering to track and vertex fitting," *Nucl. Instrum. Methods Phys. Res., A* **262** no. HEPHY-PUB-503, (Jun, 1987) 444. 19 p. https://cds.cern.ch/record/178627.

[206] T. Cornelissen, M. Elsing, I. Gavrilenko, W. Liebig, E. Moyse, and A. Salzburger, "The new ATLAS track reconstruction (NEWT)," *J. Phys.: Conf. Ser.* **119** (2008) 032014. https://cds.cern.ch/record/1176900.

[207] ATLAS Collaboration, "Vertex Reconstruction Performance of the ATLAS Detector at $\sqrt{s} = 13$ TeV." ATL-PHYS-PUB-2015-026, 2015. https://cds.cern.ch/record/2037717.

[208] ATLAS Collaboration, "Reconstruction of primary vertices at the ATLAS experiment in Run 1 proton–proton collisions at the LHC," *Eur. Phys. J. C* **77** (2017) 332, arXiv:1611.10235 [hep-ex].

[209] ATLAS Collaboration, "Topological cell clustering in the ATLAS calorimeters and its performance in LHC Run 1," *Eur. Phys. J. C* **77** (2017) 490, arXiv:1603.02934 [hep-ex].

[210] ATLAS Collaboration, "Electron and photon performance measurements with the ATLAS detector using the 2015–2017 LHC proton–proton collision data," *JINST* **14** (2019) P12006, arXiv:1908.00005 [hep-ex].

[211] ATLAS Collaboration, "Measurement of the photon identification efficiencies with the ATLAS detector using LHC Run 2 data collected in 2015 and 2016," *Eur. Phys. J. C* **79** (2019) 205, arXiv:1810.05087 [hep-ex].

[212] ATLAS Collaboration, "Electron reconstruction and identification in the ATLAS experiment using the 2015 and 2016 LHC proton–proton collision data at $\sqrt{s} = 13$ TeV," *Eur. Phys. J. C* **79** (2019) 639, arXiv:1902.04655 [hep-ex].

[213] ATLAS Collaboration, "Muon reconstruction performance of the ATLAS detector in proton–proton collision data at $\sqrt{s} = 13$ TeV," *Eur. Phys. J. C* **76** (2016) 292, arXiv:1603.05598 [hep-ex].

[214] **ATLAS** Collaboration, "Muon reconstruction and identification efficiency in ATLAS using the full Run 2 *pp* collision data set at $\sqrt{s} = 13$ TeV," arXiv:2012.00578 [hep-ex].

[215] M. Cacciari, G. P. Salam, and G. Soyez, "The anti-k_t jet clustering algorithm," *JHEP* **04** (2008) 063, arXiv:0802.1189 [hep-ph].

[216] M. Cacciari, G. P. Salam, and G. Soyez, "FastJet user manual," *Eur. Phys. J. C* **72** (2012) 1896, arXiv:1111.6097 [hep-ph].

[217] M. Cacciari, "FastJet: A Code for fast k_t clustering, and more," in *Deep inelastic scattering. Proceedings, 14th International Workshop, DIS 2006, Tsukuba, Japan, April 20-24, 2006*, pp. 487–490. 2006. arXiv:hep-ph/0607071 [hep-ph]. [,125(2006)].

[218] **ATLAS** Collaboration, G. Aad *et al.*, "Jet energy scale and resolution measured in proton-proton collisions at $\sqrt{s} = 13$ TeV with the ATLAS detector," arXiv:2007.02645 [hep-ex].

[219] M. Cacciari and G. P. Salam, "Pileup subtraction using jet areas," *Phys. Lett. B* **659** (2008) 119–126, arXiv:0707.1378 [hep-ph].

[220] ATLAS Collaboration, "Jet energy measurement with the ATLAS detector in proton–proton collisions at $\sqrt{s} = 7$ TeV," *Eur. Phys. J. C* **73** (2013) 2304, arXiv:1112.6426 [hep-ex].

[221] ATLAS Collaboration, "Determination of jet calibration and energy resolution in proton–proton collisions at $\sqrt{s} = 8$ TeV using the ATLAS detector," arXiv:1910.04482 [hep-ex].

[222] ATLAS Collaboration, "Performance of pile-up mitigation techniques for jets in *pp* collisions at $\sqrt{s} = 8$ TeV using the ATLAS detector," *Eur. Phys. J. C* **76** (2016) 581, arXiv:1510.03823 [hep-ex].

[223] ATLAS Collaboration, "Optimisation and performance studies of the ATLAS b-tagging algorithms for the 2017-18 LHC run." ATL-PHYS-PUB-2017-013, 2017. https://cds.cern.ch/record/2273281.

[224] ATLAS Collaboration, "ATLAS b-jet identification performance and efficiency measurement with $t\bar{t}$ events in pp collisions at $\sqrt{s} = 13\,\text{TeV}$," *Eur. Phys. J. C* **79** (2019) 970, arXiv:1907.05120 [hep-ex].

[225] ATLAS Collaboration, "Measurements of b-jet tagging efficiency with the ATLAS detector using $t\bar{t}$ events at $\sqrt{s} = 13\,\text{TeV}$," *JHEP* **08** (2018) 089, arXiv:1805.01845 [hep-ex].

[226] ATLAS Collaboration, "Performance of missing transverse momentum reconstruction with the ATLAS detector using proton–proton collisions at $\sqrt{s} = 13\,\text{TeV}$," *Eur. Phys. J. C* **78** (2018) 903, arXiv:1802.08168 [hep-ex].

[227] **ATLAS Collaboration** Collaboration, "$E_{\text{T}}^{\text{miss}}$ performance in the ATLAS detector using 2015-2016 LHC p-p collisions," Tech. Rep. ATLAS-CONF-2018-023, CERN, Geneva, Jun, 2018. http://cds.cern.ch/record/2625233.

[228] D. Adams *et al.*, "Recommendations of the Physics Objects and Analysis Harmonisation Study Groups 2014," Tech. Rep. ATL-PHYS-INT-2014-018, CERN, Geneva, Jul, 2014. https://cds.cern.ch/record/1743654.

[229] M. Cacciari, G. P. Salam, and G. Soyez, "The Catchment Area of Jets," *JHEP* **04** (2008) 005, arXiv:0802.1188 [hep-ph].

[230] **UA1** Collaboration, G. Arnison *et al.*, "Experimental Observation of Isolated Large Transverse Energy Electrons with Associated Missing Energy at $\sqrt{s} = 540$ GeV," *Phys. Lett. B* **122** (1983) 103–116.

[231] **Aachen-Annecy-Birmingham-CERN-Helsinki-London(QMC)-Paris(CdF)-Riverside-Rome-Rutherford-Saclay(CEN)-Vienna** Collaboration, G. Arnison *et al.*, "Further evidence for charged intermediate vector bosons at the SPS collider," *Phys. Lett. B* **129** no. CERN-EP-83-111, (Jun, 1985) 273–282. 17 p. https://cds.cern.ch/record/163856.

[232] D. R. Tovey, "On measuring the masses of pair-produced semi-invisibly decaying particles at hadron colliders," *JHEP* **04** (2008) 034, arXiv:0802.2879 [hep-ph].

[233] G. Polesello and D. R. Tovey, "Supersymmetric particle mass measurement with the boost-corrected contransverse mass," *JHEP* **03** (2010) 030, arXiv:0910.0174 [hep-ph].

[234] **ATLAS** Collaboration, G. Aad *et al.*, "Performance of the missing transverse momentum triggers for the ATLAS detector during Run-2 data taking," *JHEP* **08** (2020) 080, arXiv:2005.09554 [hep-ex].

[235] **ATLAS** Collaboration, G. Aad *et al.*, "Performance of algorithms that reconstruct missing transverse momentum in $\sqrt{s} = 8$ TeV proton-proton collisions in the ATLAS detector," *Eur. Phys. J. C* **77** no. 4, (2017) 241, arXiv:1609.09324 [hep-ex].

[236] ATLAS Collaboration, "ATLAS data quality operations and performance for 2015–2018 data-taking," *JINST* **15** (2020) P04003, arXiv:1911.04632 [physics.ins-det].

[237] ATLAS Collaboration, "Selection of jets produced in 13 TeV proton–proton collisions with the ATLAS detector." ATLAS-CONF-2015-029, 2015. https://cds.cern.ch/record/2037702.

[238] N. Hartmann, "ahoi." https://gitlab.com/nikoladze/ahoi, 2018.

[239] **ATLAS** Collaboration, "Object-based missing transverse momentum significance in the ATLAS detector," Tech. Rep. ATLAS-CONF-2018-038, CERN, Geneva, Jul, 2018. https://cds.cern.ch/record/2630948.

[240] A. Roodman, "Blind analysis in particle physics," *eConf* **C030908** (2003) TUIT001, arXiv:physics/0312102.

[241] ATLAS Collaboration, "Measurement of the Inelastic Proton–Proton Cross Section at $\sqrt{s} = 13\,\text{TeV}$ with the ATLAS Detector at the LHC," *Phys. Rev. Lett.* **117** (2016) 182002, arXiv:1606.02625 [hep-ex].

[242] ATLAS Collaboration, "A method for the construction of strongly reduced representations of ATLAS experimental uncertainties and the application thereof to the jet energy scale." ATL-PHYS-PUB-2015-014, 2015. https://cds.cern.ch/record/2037436.

[243] J. Bellm *et al.*, "Herwig 7.0/Herwig++ 3.0 release note," *Eur. Phys. J.* **C76** no. 4, (2016) 196, arXiv:1512.01178 [hep-ph].

[244] ATLAS Collaboration, "Simulation of top-quark production for the ATLAS experiment at $\sqrt{s} = 13$ TeV." ATL-PHYS-PUB-2016-004, 2016. https://cds.cern.ch/record/2120417.

[245] S. Frixione, E. Laenen, P. Motylinski, C. White, and B. R. Webber, "Single-top hadroproduction in association with a W boson," *JHEP* **07** (2008) 029, arXiv:0805.3067 [hep-ph].

[246] **ATLAS Collaboration** Collaboration, "SUSY July 2020 Summary Plot Update," Tech. Rep. ATL-PHYS-PUB-2020-020, CERN, Geneva, Jul, 2020. http://cds.cern.ch/record/2725258.

[247] **CMS Collaboration** Collaboration, "Search for chargino-neutralino production in final states with a Higgs boson and a W boson," Tech. Rep. CMS-PAS-SUS-20-003, CERN, Geneva, 2021. https://cds.cern.ch/record/2758360.

[248] ATLAS Collaboration, "Search for electroweak production of charginos and sleptons decaying into final states with two leptons and missing transverse momentum in $\sqrt{s} = 13\,\text{TeV}$ pp collisions using the ATLAS detector," *Eur. Phys. J. C* **80** (2020) 123, arXiv:1908.08215 [hep-ex].

[249] G. Apollinari, I. Béjar Alonso, O. Brüning, M. Lamont, and L. Rossi, *High-Luminosity Large Hadron Collider (HL-LHC): Preliminary Design Report*. CERN Yellow Reports: Monographs. CERN, Geneva, 2015. https://cds.cern.ch/record/2116337.

[250] **LHC Reinterpretation Forum** Collaboration, W. Abdallah *et al.*, "Reinterpretation of LHC Results for New Physics: Status and Recommendations after Run 2," *SciPost Phys.* **9** no. 2, (2020) 022, arXiv:2003.07868 [hep-ph].

[251] ATLAS Collaboration, "RECAST framework reinterpretation of an ATLAS Dark Matter Search constraining a model of a dark Higgs boson decaying to two b-quarks." ATL-PHYS-PUB-2019-032, 2019. https://cds.cern.ch/record/2686290.

[252] K. Cranmer and I. Yavin, "RECAST: Extending the Impact of Existing Analyses," *JHEP* **04** (2011) 038, arXiv:1010.2506 [hep-ex].

[253] D. Dercks, N. Desai, J. S. Kim, K. Rolbiecki, J. Tattersall, and T. Weber, "CheckMATE 2: From the model to the limit," *Comput. Phys. Commun.* **221** (2017) 383–418, arXiv:1611.09856 [hep-ph].

[254] M. Drees, H. Dreiner, D. Schmeier, J. Tattersall, and J. S. Kim, "CheckMATE: Confronting your Favourite New Physics Model with LHC Data," *Comput. Phys. Commun.* **187** (2015) 227–265, arXiv:1312.2591 [hep-ph].

[255] E. Conte, B. Fuks, and G. Serret, "MadAnalysis 5, A User-Friendly Framework for Collider Phenomenology," *Comput. Phys. Commun.* **184** (2013) 222–256, arXiv:1206.1599 [hep-ph].

[256] E. Maguire, L. Heinrich, and G. Watt, "HEPData: a repository for high energy physics data," *J. Phys. Conf. Ser.* **898** no. 10, (2017) 102006, arXiv:1704.05473 [hep-ex].

[257] **ATLAS** Collaboration, "Simpleanalysis." https://gitlab.cern.ch/atlas-sa/simple-analysis, 2021.

[258] S. Ovyn, X. Rouby, and V. Lemaitre, "DELPHES, a framework for fast simulation of a generic collider experiment," arXiv:0903.2225 [hep-ph].

[259] A. Buckley, J. Butterworth, D. Grellscheid, H. Hoeth, L. Lonnblad, J. Monk, H. Schulz, and F. Siegert, "Rivet user manual," *Comput. Phys. Commun.* **184** (2013) 2803–2819, arXiv:1003.0694 [hep-ph].

[260] A. Buckley, D. Kar, and K. Nordström, "Fast simulation of detector effects in Rivet," *SciPost Phys.* **8** (2020) 025, arXiv:1910.01637 [hep-ph].

[261] S. Kraml, S. Kulkarni, U. Laa, A. Lessa, W. Magerl, D. Proschofsky-Spindler, and W. Waltenberger, "SModelS: a tool for interpreting simplified-model results from the LHC and its application to supersymmetry," *Eur. Phys. J. C* **74** (2014) 2868, arXiv:1312.4175 [hep-ph].

[262] F. Ambrogi, S. Kraml, S. Kulkarni, U. Laa, A. Lessa, V. Magerl, J. Sonneveld, M. Traub, and W. Waltenberger, "SModelS v1.1 user manual: Improving simplified model constraints with efficiency maps," *Comput. Phys. Commun.* **227** (2018) 72–98, arXiv:1701.06586 [hep-ph].

[263] **ATLAS** Collaboration, "Search for direct production of electroweakinos in final states with one lepton, missing transverse momentum and a higgs boson decaying into two b-jets in pp collisions at $\sqrt{s} = 13$ tev with the atlas detector," 2021. https://www.hepdata.net/record/ins1755298?version=4.

[264] **ATLAS** Collaboration, "1lbb-likelihoods-hepdata.tar.gz," 2020. https://www.hepdata.net/record/resource/1408476?view=true.

[265] G. Alguero, S. Kraml, and W. Waltenberger, "A SModelS interface for pyhf likelihoods," arXiv:2009.01809 [hep-ph].

[266] M. D. Goodsell, "Implementation of the ATLAS-SUSY-2019-08 analysis in the MadAnalysis 5 framework (electroweakinos with a Higgs decay into a $b\bar{b}$ pair, one lepton and missing transverse energy; 139 fb^{-1})," *Mod. Phys. Lett. A* **36** no. 01, (2021) 2141006.

[267] J. Y. Araz *et al.*, "Proceedings of the second MadAnalysis 5 workshop on LHC recasting in Korea," *Mod. Phys. Lett. A* **36** no. 01, (2021) 2102001, arXiv:2101.02245 [hep-ph].

[268] M. Feickert, L. Heinrich, G. Stark, and B. Galewsky, "Distributed statistical inference with pyhf enabled through funcX," in *25th International Conference on Computing in High-Energy and Nuclear Physics*. 3, 2021. arXiv:2103.02182 [cs.DC].

[269] R. Chard, Y. Babuji, Z. Li, T. Skluzacek, A. Woodard, B. Blaiszik, I. Foster, and K. Chard, "funcx: A federated function serving fabric for science," ACM, Jun, 2020. http://dx.doi.org/10.1145/3369583.3392683.

[270] D. Merkel, "Docker: Lightweight linux containers for consistent development and deployment," *Linux J.* **2014** no. 239, (Mar., 2014) .

[271] S. Binet and B. Couturier, "docker & HEP: Containerization of applications for development, distribution and preservation," *J. Phys.: Conf. Ser.* **664** no. 2, (2015) 022007. 8 p. https://cds.cern.ch/record/2134524.

[272] K. Cranmer and L. Heinrich, "Yadage and Packtivity - analysis preservation using parametrized workflows," *J. Phys. Conf. Ser.* **898** no. 10, (2017) 102019, arXiv:1706.01878 [physics.data-an].

[273] ATLAS Collaboration, "Electron and photon energy calibration with the ATLAS detector using 2015–2016 LHC proton–proton collision data," *JINST* **14** (2019) P03017, arXiv:1812.03848 [hep-ex].

[274] ATLAS Collaboration, "Searches for electroweak production of supersymmetric particles with compressed mass spectra in $\sqrt{s} = 13\,\text{TeV}$ pp collisions with the ATLAS detector," *Phys. Rev. D* **101** (2020) 052005, arXiv:1911.12606 [hep-ex].

[275] ATLAS Collaboration, "Search for direct stau production in events with two hadronic τ-leptons in $\sqrt{s} = 13\,\text{TeV}$ pp collisions with the ATLAS detector," *Phys. Rev. D* **101** (2020) 032009, arXiv:1911.06660 [hep-ex].

[276] ATLAS Collaboration, "Search for bottom-squark pair production with the ATLAS detector in final states containing Higgs bosons, b-jets and missing transverse momentum," *JHEP* **12** (2019) 060, arXiv:1908.03122 [hep-ex].

[277] Schanet, Eric, "simplify: v0.1.5." https://github.com/eschanet/simplify.

[278] W. Porod, "SPheno, a program for calculating supersymmetric spectra, SUSY particle decays and SUSY particle production at e+ e- colliders," *Comput. Phys. Commun.* **153** (2003) 275–315, arXiv:hep-ph/0301101.

[279] W. Porod and F. Staub, "SPheno 3.1: Extensions including flavour, CP-phases and models beyond the MSSM," *Comput. Phys. Commun.* **183** (2012) 2458–2469, arXiv:1104.1573 [hep-ph].

[280] S. Heinemeyer, W. Hollik, and G. Weiglein, "FeynHiggs: A Program for the calculation of the masses of the neutral CP even Higgs bosons in the MSSM," *Comput. Phys. Commun.* **124** (2000) 76–89, arXiv:hep-ph/9812320.

[281] H. Bahl, T. Hahn, S. Heinemeyer, W. Hollik, S. Paßehr, H. Rzehak, and G. Weiglein, "Precision calculations in the MSSM Higgs-boson sector with FeynHiggs 2.14," *Comput. Phys. Commun.* **249** (2020) 107099, arXiv:1811.09073 [hep-ph].

[282] T. Hahn, S. Heinemeyer, W. Hollik, H. Rzehak, and G. Weiglein, "High-Precision Predictions for the Light CP -Even Higgs Boson Mass of the Minimal Supersymmetric Standard Model," *Phys. Rev. Lett.* **112** no. 14, (2014) 141801, arXiv:1312.4937 [hep-ph].

[283] B. C. Allanach, "SOFTSUSY: a program for calculating supersymmetric spectra," *Comput. Phys. Commun.* **143** (2002) 305–331, arXiv:hep-ph/0104145 [hep-ph].

[284] G. Belanger, F. Boudjema, A. Pukhov, and A. Semenov, "MicrOMEGAs 2.0: A Program to calculate the relic density of dark matter in a generic model," *Comput. Phys. Commun.* **176** (2007) 367–382, arXiv:hep-ph/0607059.

[285] G. Belanger, F. Boudjema, A. Pukhov, and A. Semenov, "micrOMEGAs: A Tool for dark matter studies," *Nuovo Cim. C* **033N2** (2010) 111–116, arXiv:1005.4133 [hep-ph].

[286] W. Beenakker, R. Hopker, and M. Spira, "PROSPINO: A Program for the Production of Supersymmetric Particles in Next-to-leading Order QCD," Tech. Rep. hep-ph/9611232, Nov, 1996. https://cds.cern.ch/record/314229. 12 pages, latex, no figures, Complete postscript file and FORTRAN source codes available from http://wwwcn.cern.ch/ mspira/prospino/.

[287] W. Beenakker, M. Klasen, M. Kramer, T. Plehn, M. Spira, and P. M. Zerwas, "The Production of charginos / neutralinos and sleptons at hadron colliders," *Phys. Rev. Lett.* **83** (1999) 3780–3783, arXiv:hep-ph/9906298. [Erratum: Phys.Rev.Lett. 100, 029901 (2008)].

[288] **ATLAS Collaboration** Collaboration, "Search for long-lived charginos based on a disappearing-track signature using 136 fb^{-1} of pp collisions at $\sqrt{s} = 13$ TeV with the ATLAS detector," Tech. Rep. ATLAS-CONF-2021-015, CERN, Geneva, Mar, 2021. https://cds.cern.ch/record/2759676.

[289] A. Arbey, M. Battaglia, and F. Mahmoudi, "Higgs Production in Neutralino Decays in the MSSM - The LHC and a Future e^+e^- Collider," *Eur. Phys. J. C* **75** no. 3, (2015) 108, arXiv:1212.6865 [hep-ph].

[290] M. E. Cabrera, J. A. Casas, A. Delgado, S. Robles, and R. Ruiz de Austri, "Naturalness of MSSM dark matter," *JHEP* **08** (2016) 058, arXiv:1604.02102 [hep-ph].